A Technology Assessment of

Nondestructive Evaluation (NDE) of Advanced Fiber Reinforced Polymer Composites

NTIAC-TA-01-01

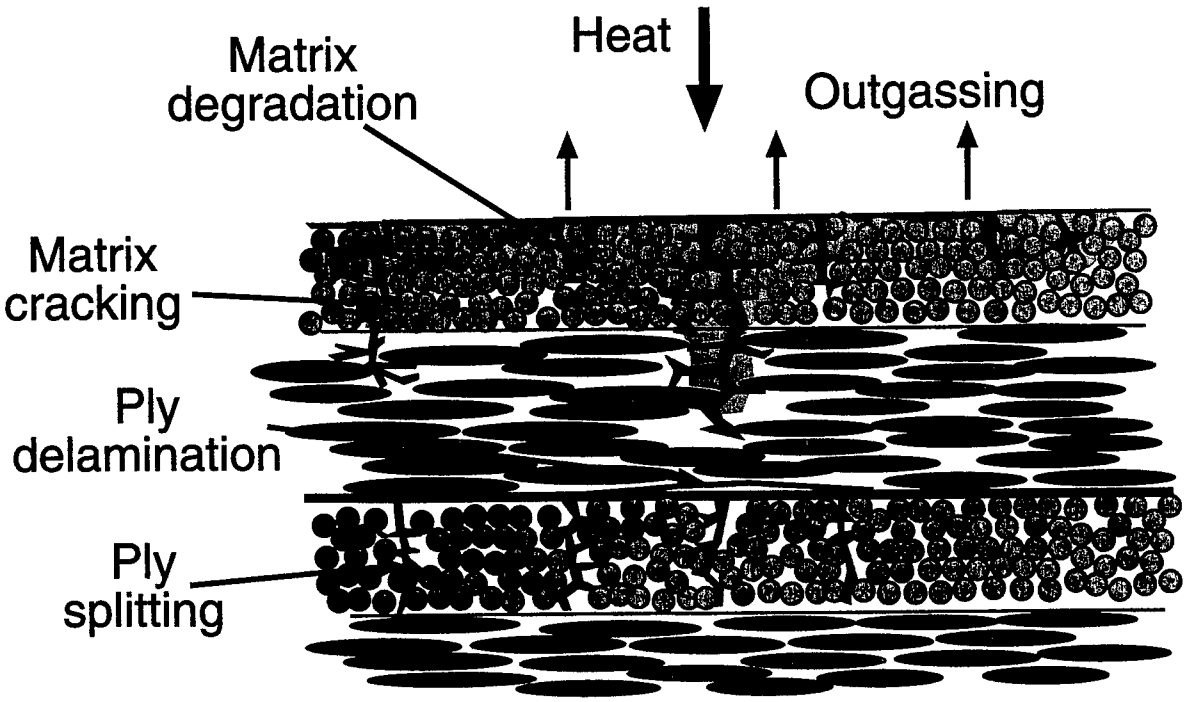

Thermal Damage in Laminated Composites

NTIAC

Nondestructive Testing Information Analysis Center
A DoD Information Analysis Center Sponsored by the
Defense Technical Information Center (DTIC)

July 2001

This document was prepared by the Nondestructive Testing Information Analysis Center (NTIAC), TRI/Austin, Inc., 415 Crystal Creek Drive, Austin, TX 78746-4725. NTIAC is a full service information analysis center operated under Contract SPO700-97-D-4003 for the U.S. Department of Defense, serving the information needs of the Department of Defense, other U.S. Government agencies, and the private sector in the field of nondestructive testing.

NTIAC is sponsored by the Defense Technical Information Center (DTIC) and administered by the Defense Information Systems Agency (DISA). Technical aspects of NTIAC operations are monitored by the Office of the Deputy Undersecretary of Defense (S&T).

Additional copies of this document may be obtained from:

NTIAC
415 Crystal Creek Drive
Austin, TX 78746-4725
Phone: (512) 263-2106 or (800) NTIAC 39
Fax: (512) 263-3530
E-mail: info@ntiac.com

ISBN 1-890596-19-1

NTIAC-TA-01-01

A Technology Assessment of

Nondestructive Evaluation (NDE) of Advanced Fiber Reinforced Polymer Composites

By

H. Thomas Yolken

George A. Matzkanin

and

Jill E. Bartel

Nondestructive Testing Information Analysis Center
A DTIC-Sponsored DoD Information Analysis Center
Operated by TRI/Austin, Inc., *A Texas Research International Company*

July 2001

CONTENTS

List of Figures

List of Tables

Preface

This Technology Assessment was prepared under NTIAC Contract No. SPO700-97-D-4003 which is funded by the Defense Technical Information Center (DTIC). A portion of this report had been prepared for the National Institute of Standards and Technology (NIST) under Contract No. 50-DKNB-0-90095 and was included as Appendix B in the Final Report for that project. Appendix B was expanded and additional documents reviewed for inclusion in this Technology Assessment.

1.0 INTRODUCTION

Fiber reinforced polymer composite materials continue to be used in a large number of applications ranging from aerospace to automotive, industrial and consumer products. The high stiffness-to-weight ratio, low electromagnetic reflectance, and the ability to embed sensors and actuators have made fiber reinforced composites an attractive alternative construction material for primary aircraft structures. In many other cases fiber reinforced polymer composite materials are being developed and used to replace metal components, in particular in corrosive environments.

Because of their increasing utilization in structural applications, the nondestructive evaluation (NDE) of fiber reinforced polymer composites continues to receive considerable research and development attention. Due to the heterogeneous nature of composites, the form of defects is often very different from a metal and fracture mechanisms are more complex. The purpose of this report is to provide an overview and technology assessment of the current state-of-the-art with respect to NDE of fiber reinforced polymer composites. Approximately 100 documents identified through literature searches of various data bases were reviewed and summarized into the information presented in the following sections. Background information is provided in Section 2 not only on "conventional" fiber reinforced polymer composites but also on newer hybrid composite materials. The current status of NDE technologies for the most prominent defect conditions in fiber reinforced polymer composites is presented in Section 3 and Conclusions and Prognosis are presented in Section 4. Besides the list of references used in the text of the report, an extensive list of additional relevant documents is included in a Bibliography.

2.0 BACKGROUND

2.1 Fiber Reinforced Polymer Composites

The advantages of advanced composite materials in modern structures are well known: strength, stiffness, lightweight, and corrosion resistance (Eihusen and Peters 1999). Typical aerospace applications for advanced composites are ultra-high-performance pressure vessels, rocket motor cases, and launch tubes. Aeronautical applications include helicopter rotor blades and external fuel tanks for combat aircraft. Commercial applications cover a wide range of uses including bike frames, tennis rackets, fuel containers used to store compressed natural gas for motor vehicles, and high-performance tubular products used in the offshore oil and gas industry.

A fundamental reason for the popularity of advanced composite materials is the flexibility that is presented to a designer in tailoring the material properties to the application. This is achieved by selection of the resin matrix and fiber reinforcement to yield the desired response in the finished structure (Eihusen and Peters 1999).

Composite materials are formed by combining two or more materials that have quite different properties, so that the different materials work together to give the composite its unique properties. In general, composite materials are very durable; the right composites stand up well to heat, corrosion, and cyclic loading. Another advantage of composite materials is that they can be molded into complex shapes, and designers can reduce the number of small parts in a system by combining several small parts into one larger composite component. The disadvantages of advanced composites are the cost, the manufacturing processes tend to be complex, and the nondestructive evaluation of parts during and after manufacture or in-service is often more difficult than with conventional homogenous metals, polymers, and ceramics.

Glass fibers, by far the most common reinforcement, are made of silicon oxide with the addition of small amounts of other oxides. These fibers generally have high tensile strength, good temperature and corrosion resistance, and low price. However, the glass fibers are also brittle and will break if bent sharply. There are two main types of glass fibers: E-glass and S-glass. E-glass fibers are the most used and are named after their good electrical properties. S-glass fibers are very strong (hence the name), stiff, and temperature resistant. The fibers are produced by a spinning process, in which they are pulled through a nozzle from molten glass at the rate of thousands of meters per second. Glass fibers are used as reinforcing materials in many composite applications; for example car bodies and panels, boat hulls, swimming pool liners and surf boards.

Carbon fibers are the stiffest and strongest reinforcing fibers for polymer composites, and, after glass fibers, are the most used. Made of pure carbon in the form of graphite, these fibers have low density and a negative coefficient of longitudinal thermal expansion. However, the drawbacks are that carbon fibers are very expensive and can produce galvanic corrosion when in contact with metals. Carbon fibers are produced by either the PAN or the pitch method. The PAN method separates a chain of carbon atoms

from polyacrylnitrile (PAN) through heating and oxidation. The pitch method pulls out graphite threads through a nozzle from hot fluid pitch. Carbon fibers are generally used with epoxy, where high strength and stiffness are required. Carbon fiber reinforced polymer composites find uses in, for example, racecars, automotive, aeronautical, aerospace, and medical applications (to repair or replace damaged bones), and sports equipment.

Epoxy is a strong and very resistant thermoset polymer (also called a resin). (The use of plastics in the matrix explains the name "reinforced plastics" commonly given to composites.) Curing of the epoxy takes place by adding a hardening agent. The type of hardener used has a major influence on the properties and applications of epoxies. Epoxy is resistant to almost all acids and solvents, but not to strong bases or solvents with chlorine content. It is used as an adhesive agent, as filling material, for molding dies, and as a protective coating on steel and concrete. Many polymer composite materials have an epoxy matrix.

2.2 Hybrid Composites

Hybrid composites are those composites that have a combination of two or more reinforcement materials (continuous or fragments) in a matrix or binder. This type of composite is usually used when a combination of properties provided by different types of fibers is desired, or when longitudinal as well as lateral mechanical performances are required. The most common hybrid composites are carbon-aramid-reinforced epoxy (which combines strength and impact resistance) and glass-carbon-reinforced epoxy (which gives a strong material at a more reasonable price than using only carbon fibers).

Mixing or hybridizing different types of reinforcement fibers within a structure can be accomplished in two ways: 1) interply hybridization, where layers (lamina) of different fiber types are laminated together, and 2) intraply hybridization, where different fiber types are mixed within the individual layers (lamina) (Eihusen and Peters 1999). In interplay hybridization (see Figure 2.2-1) each layer of material is stacked to provide the required response in the structure. An example of this type of hybridization is the use of high- and low-modulus fibers to tailor the radial strain gradient in very high-pressure storage containers.

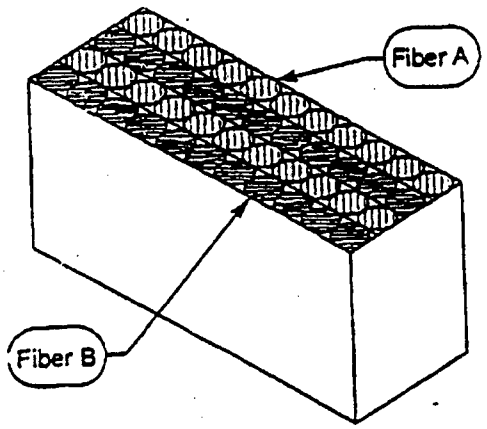

Figure 2.2-1. Interply hybrid laminate. (Eihusen and Peters 1999)

Intraply hybridization (see Figure 2.2-2) finds many applications in long fiber composites fabricated by braiding or filament winding (Eihusen and Peters 1999). With these types of composite fabrication it is most convenient to use spools of different fiber reinforcements in the same manner as threads of different colors are woven into common cloth.

Hybrid materials are commonly pultruded, filament wound, or vacuum infused, and often contain mat. Matrix materials are typically epoxy, vinyl ester, or polyurethane. Fiber reinforcement orientations vary from unidirectional to four directions. An everyday example of a hybrid composite (glass-carbon-reinforced epoxy) is bicycle frames. While there are a variety of hybrid composites, one of the most common types are those hybrids that contain both carbon and glass fibers in a single, graphite-epoxy matrix.

The number of design variables and the interaction of the constituents of the composite system complicate the design of hybrid composite structures. As a quality assurance procedure, it would be of great value to verify the fiber directions, porosity and fiber content in a hybrid composite in order to evaluate the overall properties of a composite structure.

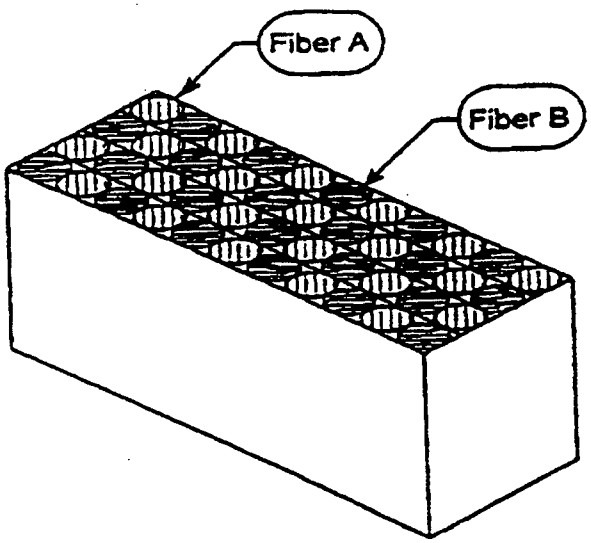

Figure 2.2-2. Intraply hybrid laminate.
(Eihusen and Peters 1999)

3.0 NDE OF COMPOSITES

3.1 General Information

Composite materials represent acoustically and thermally heterogeneous materials where a variety of defects with different dimensions may be formed. Typical defects of composite materials include fiber breaks, microcracks, microsplits, foreign objects, and pores in the bonding medium, and detachment of fibers from the bonding material. Fiber waviness, fiber direction and fiber ratio (in hybrids) are also important microstructural properties of composites. Many of these defects or microstructural variations result in changes of the acoustic attenuation and the speed of sound in composite materials. That is why ultrasonic nondestructive evaluation is currently one the most frequently used methods for nondestructive evaluation of polymer matrix composites. Many of these defects and microstructural changes also result in changes in the thermal properties of the material and thermography is also used to inspect polymer composites.

Many of the current nondestructive evaluation (NDE) techniques for composites have been developed for the inspection of relatively thin, graphite composites. While some successes have been reported with ultrasound applied to thick section composites, in general the large apparent attenuation dictates the use of relatively low-frequency (1 MHz or lower) transducers of relatively large physical size, thereby reducing depth resolution (Liu 1998). It is difficult to reliably detect near-surface defects using this type of transducer. The relatively large signal attenuation can be attributed to the coherent scattering from the coarse microstructure and existence of voids in thick sections. This scattering produces a coherent "noise" signal that returns before the backwall signal, making it difficult to detect defects in some situations.

However, mainly because of geometric effects and fiber architecture, current nondestructive evaluation techniques ranging form immersion ultrasonics, to x-ray radioscopy are not providing the feedback needed to confidently predict structural integrity and service life of composite parts (Reis 1994). These NDE techniques are also often time-consuming and operator-dependent.

Interest has been shown in developing microwave and millimeter wave NDE techniques for glass-reinforced plastics (GRPs). Microwaves scatter from the coarse microstructure and voids, but because of the much lower impedance mismatch between air and material, the scattering is reduced when compared to ultrasound. However, microwave techniques are of limited use in composites containing graphite fibers that are electrically conducting. Electrically conducting material as contrasted to dielectric material, scatters the microwaves – similar to the reason why metal containers should not be used in a microwave oven.

For quantitative microstructural characterization, more detailed knowledge of the mathematical relationships between the properties of the constituent materials and the resulting composite structure are required (Kline 1991).

The ever-increasing demand for higher quality composite materials has driven engineers to improve manufacturing processes and inspection of the product. For some manufacturing methods, in-process inspection may provide a means to improve quality and efficiency. Continuous composite manufacturing processes, such as pultrusion, are ideal candidates for in-process inspection. In a continuous process, the consolidated composite passes a common location at a particular point in the manufacturing cycle. A nondestructive evaluation station placed at that location would thus have the capability of 100% inspection of the finished product (Fecko et al. 1996).

In-situ NDE must be done quickly to keep up with the manufacturing process. Thus, in this situation, a quick measurement of bulk ultrasonic properties is preferable to measuring the same property at each point on the sample and building up an image based on the individual responses as in ultrasonic C-scan testing (Fecko et al. 1995). Attenuation, and longitudinal and shear wave velocities all provide for measurements of bulk materials properties and have been used to measure porosity in various composite materials. For a more detailed discussion of NDE for polymer composite process see NTIAC-TA-98-02, A Technology Assessment of NDE for Process Control of Polymer Composite Fabrication, October 1998.

Analytical ultrasonics implies the measurement of material microstructure and associated factors that govern material properties such as mechanical properties and dynamic response. It goes beyond flaw detection, flaw imaging, and defect characterization and includes assessing the inherent properties of materials in which the flaws reside (Reis 1994a). Acousto-ultrasonics is an analytical ultrasonic NDE technique that provides an integrated bulk measurement of the relative efficiency of energy transmission in the specimen. When applied to composites, this approach allows perturbations in the material structure to be identified by measuring perturbations in specific waveform features, commonly referred as stress wave factors (SWFs) (Reis 1994b).

3.2 Porosity

Porosity, in the form of distributed voids, is a perennial problem in composite manufacturing, especially for laminated structures such as carbon-fiber-reinforced polymer composites. Porosity in conventional and hybrid composites may be the result of a number of conditions, including:

- Improper conditions when manufactured
- Uneven wetting of the fibers
- Incomplete chemical reactions
- Inappropriate chemical reactions
- Degassing of contaminates (such as oils and silicones)
- Improper debulking leaving air trapped between the plies
- Poor ventilation restricting the removal of any degassing of the panel.

No matter what the source, porosity can have a detrimental effect on the performance of the structure by leaving regions of unsupported fibers and points of stress concentration (Walker et al. 1998). An increase in porosity leads to a decrease in density, modulus, and strength of the composite.

The term porosity as applied to composite laminates generally refers to the voids caused by trapped air or volatile gas released during the cure process. The larger voids within a ply are usually small and spherical. The size and shape and distribution of the voids depend on the structure of the composite. The presence of porosity has been shown to have a strong correlation with certain mechanical strength measures. Matrix-dominated features such as compressive strength, transverse tensile strength, and interlaminar shear strength are affected the most (Hsu 1988; Hsu 1995). If the regions of porosity are large enough, they may begin to interlink under stress and drastically weaken the load carrying capability of the fibers especially when put under compressive forces (Walker et al. 1998).

Determining porosity level (or the amount of void content) in cured conventional and hybrid composite materials is an important practical issue. Void content is often regarded as a measure of quality by the composites industry. In composites, the porosity can be within the matrix material, which will affect the performance in a similar fashion to those in bulk materials. However, porosity often concentrates at specific locations in composite materials (either between plies or at the fiber/matrix interface), and can dramatically lower flexural and shear performance. Increases in porosity during operation (material under loading) may precede macroscopic damage and possibly indicate the presence of delamination. Hence, a nondestructive evaluation technique capable of detecting and accurately determining porosity level in materials is desirable. (Gray et al. 1995).

Techniques for detecting porosity in composite materials may be broadly categorized as one of the following: direct imaging; correlation with a single ultrasonic frequency (narrowband approach); or correlation with ultrasonic frequency slope (broadband approach) (McRae and Zala 1995). Direct imaging of the porosity may be used if the pore size is sufficiently large (greater than the resolution cell size of the ultrasonic image). This technique may require additional image processing and can be difficult to quantify. Of the two empirical correlation techniques, correlation of the frequency slope of the attenuation curve has been successfully demonstrated and has been widely applied. It has been demonstrated experimentally that there is an approximately linear relation between attenuation and frequency for graphite-epoxy composites containing porosity. There also appears to be an approximately linear variation of slope as a function of increasing void content.

Hsu (1988) used through-transmission ultrasonics to determine the void content (volume percent) of a carbon-fiber-reinforced plastic (CFRP). The void content is directly proportional to the slope of attenuation with respect to frequency, also known as the attenuation slope. The constants of proportionality depend on the shape of the voids and the elastic properties of the laminate. Frequency dependent attenuation was obtained in

the 2 to 16 MHz range on carbon-epoxy and carbon-polyimide composites containing up to 12% voids in woven laminates and up to 6% voids in nonwoven unidirectional and quasi-isotropic laminates. In modeling the porosity-induced attenuation, the pores in CFRP laminates made from unidirectional prepregs are modeled as long cylindrical cavities with elliptical cross sections. For woven laminates, the voids are mostly spherical.

Using the correlation between void content and the attenuation slope, Hsu ultrasonically determined void contents and compared them with void contents determined destructively by acid digestion. Figure 3.2-1 shows the results for nonwoven carbon-epoxy laminates and Figure 3.2-2 shows the results for woven carbon epoxy laminates. It should be pointed out that the good agreement for carbon epoxy laminates shown in Figure 3.2-2 was obtained using correlation constants determined from carbon polyimide laminates. Since the matrix materials were different and so were the weave structures, this indicates that the method is not very sensitive to material variability. In addition, the correlation constants established by using sets of thin coupons (2 to 3 mm) containing different amounts of voids were found to give good void content estimates in much thicker coupons (up to 12.7 mm).

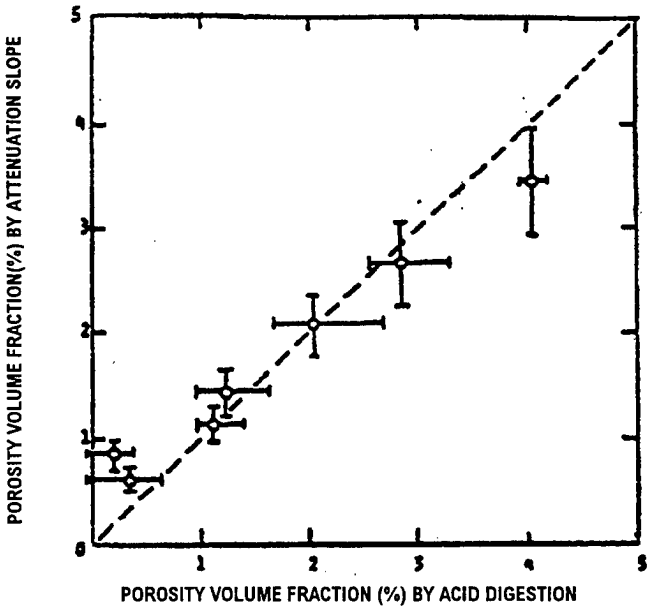

Figure 3.2-1. Comparison of ultrasonically determined void content in carbon-epoxy laminates made from unidirectional prepregs with void content determined by acid digestion.
(Hsu 1988)

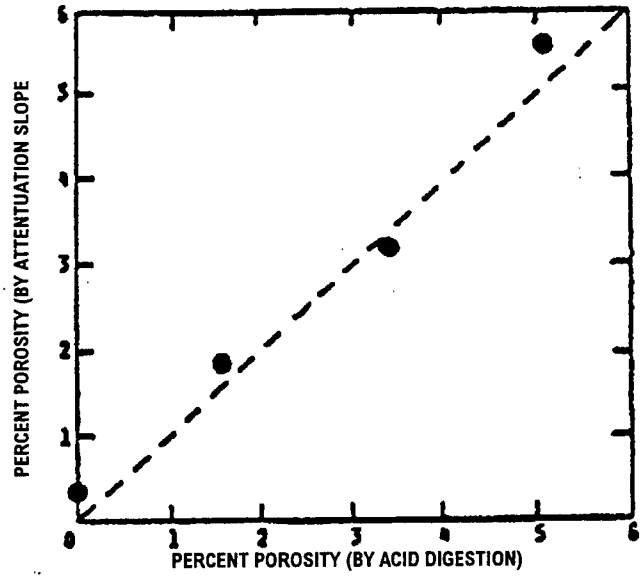

Figure 3.2-2. Comparison of ultrasonically determined void contents in woven carbon-epoxy laminates with those determined by acid digestion. (Hsu 1988)

In order to determine the amount of porosity, Steiner (1992) used ultrasonic pulse-echo C-scan imaging to study composite panels with various porosity contents. The samples ranged from 1.17% to 3.57% porosity and had a thickness of about 2-mm. A 15-MHz transducer with a scan increment of 0.23 mm was chosen for use on a robotic ultrasonic inspection system (see Figure 3.2-3). The ultrasonic receiver gain was selected such that none of the resulting C-scan images (histograms) were either over- or under-saturated. Subsections of the porosity panels were subjected to digitized full-volume waveform analysis. A useful feature of the full-waveform analysis program is the ability to produce two-dimensional waveform histograms. Superimposing all individually digitized waveforms generates these histograms. The resulting image gives a clear indication of the waveform distribution and of occurring abnormalities. Figure 3.2-4 compares two 2-dimensional waveform histograms relating to a sample with low porosity (0.17%) and a sample with high porosity (3.57%). The low-porosity sample shows almost no echo activity between the front and the back echo, whereas the high-porosity sample features a dramatic increase in echo activity between front and back echoes, thus reducing the back echo.

This technique demonstrates the influence of voids on the ultrasonic waveform. These porosity studies were directed towards qualitative rather than quantitative results. In order to use ultrasonic NDE techniques to measure the porosity contents, it will be necessary to establish a database by preparing and measuring an appropriate number of samples with known void contents and then to relate future scan data to the established database (Steiner 1992).

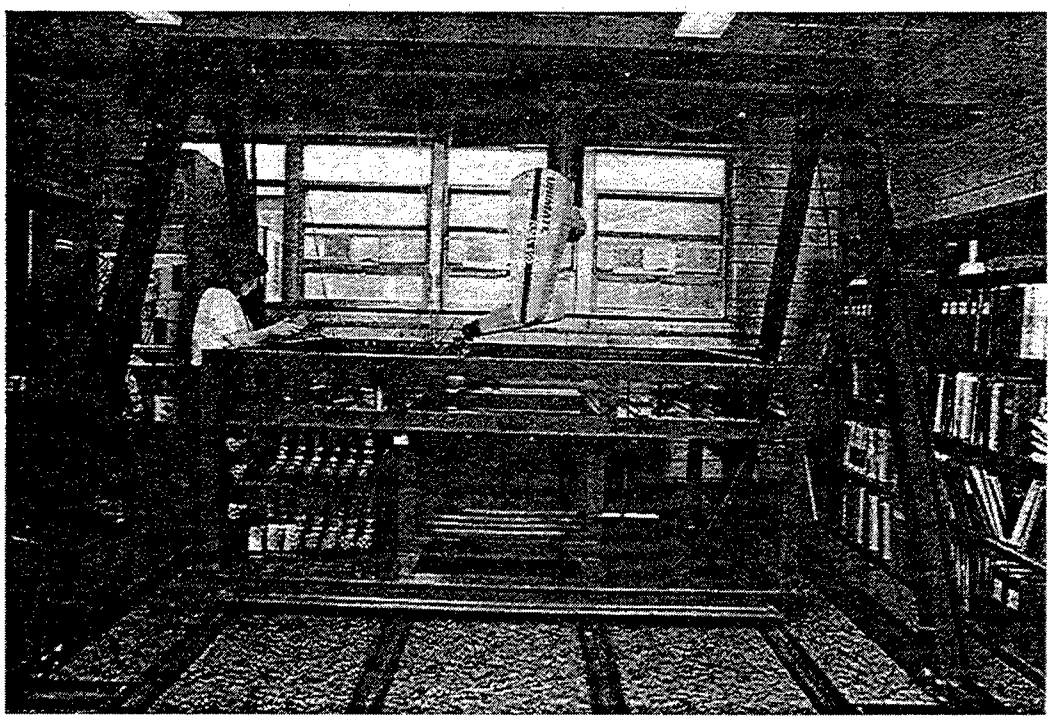

Figure 3.2-3. Robotic ultrasonic nondestructive workstation (Steiner 1992)

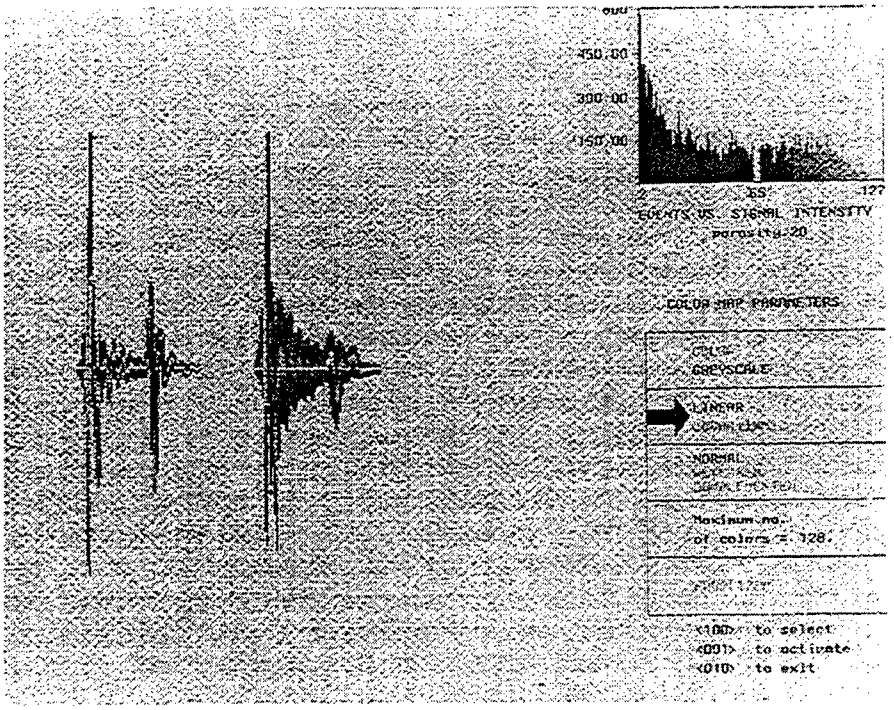

Figure 3.2-4. Two-dimensional waveform histograms for the 0.17% porosity sample (left) and the 3.57% porosity sample (right). (Steiner 1992)

Akers et al. (1996) used a reflected through-transmission ultrasonic technique to determine the void volume fraction (porosity) of composite panels made from graphite/BMI tape and fabric, graphite/epoxy tape and fabric, and glass/BMI fabric. Each material sample was ultrasonically C-scanned with full RF waveforms. The information was collected according to material-specific standards with known gain settings and stored to optical disk. The full RF waveforms were then processed using a fast Fourier transform (FFT) and the tabulated data was used to calculate the frequency response. Unfortunately, the bias voltage of the software program introduced a systematic error of approximately ±2% in the attenuation data, whereas a statistical error of 4% to 5% exists from the approximation in determining the central frequency at -6 dB from the peak frequency of the FFT waveform. Ultimately, a total uncertainty of 25% exists in the attenuation slope.

The mean ultrasonic attenuation was plotted as a function of frequency for samples of varying levels of porosity. The attenuations of the epoxy fabric and the BMI tape samples are fairly linear functions of frequency. The presence of porosity in laminates not only affects the attenuation slope, but also the frequency content of the waveform shifts due to scattering of the sound by the pores. Akers et al. showed that the higher frequencies are scattered more than the lower frequencies, resulting in a greater attenuation at the higher end of the spectrum. After analyzing a broad database of ultrasonic information for a variety of materials, they showed that the average percent void content can be given as a function of either attenuation slope or normalized shift of the central frequency due to the porosity present. Akers et al. believe this technique could be applied to non-flat laminates by processing real-time FFTs during the acquisition mode of a scan, searching a CATIA model of the part for thicknesses, and checking a given material look-up-table for attenuation slope or shift in centroid frequency. These applications would reduce the time needed for multiple C-scans of a part with complex geometry.

Fecko et al. (1995) investigated the ability of Lamb waves and acousto-ultrasonic waves to predict porosity using rolling contact transducers to send and receive the ultrasonic signals in a pultruded thermoplastic matrix composite. These inspection techniques used two transducers positioned at normal incidence to the composite in a through-transmission mode to generate and receive ultrasonic waves that propagate through the sample (see Figure 3.2-5). The ultrasonic signals were analyzed for Lamb wave velocity and for acousto-ultrasonic stress wave factors. Careful processing (done off-line) of the waveform data revealed the degree of porosity in the composite samples. The velocity of Lamb waves was shown to be linear with void content and could therefore be used to accurately measure porosity. Fecko et al. performed a series of in-situ tests on an actual laboratory scale pultrusion process, which accurately predicted the porosity in a 6.4-mm x 3.2-mm (0.25-inch x 0.125-inch) dross section pultruded rod over a range of 0.5% to 12% void volume fraction. Acousto-ultrasonic stress wave factor, on the other hand, was not measured accurately using the rolling contact transducers due to fluctuations in signal sensitivities.

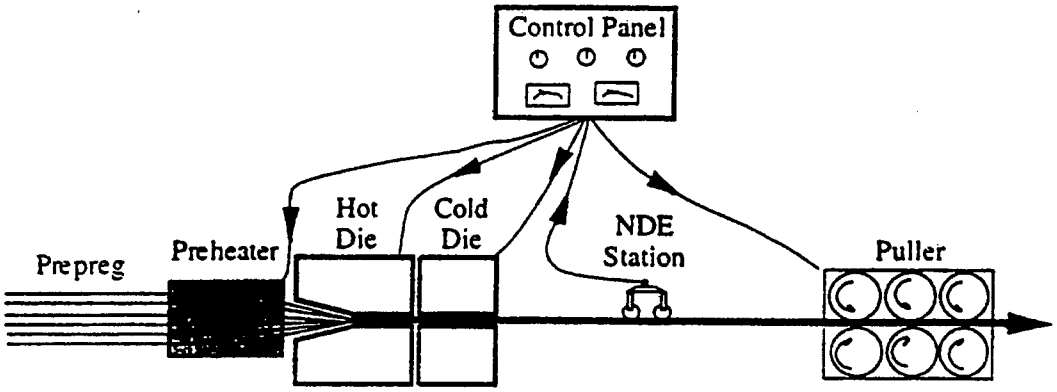

Figure 3.2-5. Schematic view of the thermoplastic pultrusion and inspection process.
(Fecko et al. 1995)

Looking to quantify defects such as porosity and delaminations in complex structural components, Reis (1994a; 1994b) demonstrated the feasibility of the acousto-ultrasonic approach as a quantitative NDE technique for porosity content in laminated composites. Four panels of PMR-15 resin reinforced with T-300 graphite fibers were manufactured with different porosities and seeded defects. The laminates had a 14-ply stacking sequence (0, +45,0, 0, -45, 0, -45, +45, 0, +45, 0, 0, -45, 0) with six zero plies added on each side. The panels were then machined into flange radii samples. The specimens were initially inspected using an ultrasonic through-transmission method to quantify porosity content, and C-scans were obtained to verify the location of simulated defects. The porosity levels ranged from <2% to >6%.

In the test setup, both the transmitting and the receiving transducers were mounted on the same side of the test specimen (see Figure 3.2-6). A 0.4-mm layer of silicone rubber was attached to the end of the waveguide and used as a dry couplant. Stress wave factor (SWF) measurements were recorded for each sample. Five waveforms were collected every 10° from 0° to 360°. The seeded defects (3.2-mm diameter shims) were not detected since they did not produce significant change in the waveform, and therefore the stress wave factors remained relatively constant.

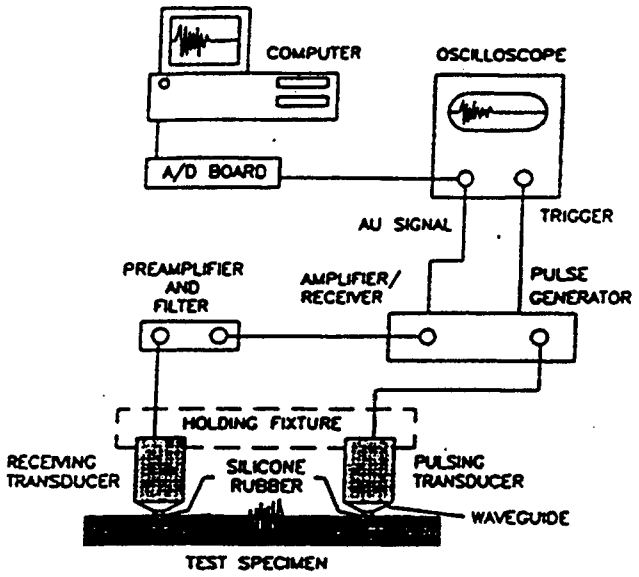

Figure 3.2-6. Typical instrument arrangement for acousto-ultrasonic measurements.
(Reis 1994a)

Reis demonstrated that the acousto-ultrasonic approach allows the quantitative discrimination of different porosity levels in flange radii components, which are typical of complex structural parts made of advanced composite materials. Not only is the correlation to porosity established, but the relationship between the SWF and fiber orientation for a given porosity is also retained.

Because ultrasonic testing is time consuming and often requires submersion in a water tank during scanning, this method is not always well suited for in-service inspections. In an effort to determine the potential for an infrared thermographic inspection method to replace ultrasonic testing, Walker et al. (1998) conducted a series of tests on graphite-epoxy composite aircraft instrumentation racks. A section of a rack panel with known porosity was inspected thermographically and compared against the ultrasonic results. The ultrasonic imaging showed the porosity in the complete thickness of the panel while the thermogram showed only the effects from a single slice of the cross section. When several thermograms were viewed over time, by rastering through the scan history, most if not all of the details in the ultrasonic image could be seen in the thermography image.

A successful thermal inspection requires that heat be introduced into a structure uniformly and with sufficient intensity to create a temporary thermal imbalance around an anomaly as well as to resolve those temperature variations. In the author's experimental arrangement, the surface of the test object must be "black" and dull to absorb the heat from the flash lamps. It may be necessary to apply a flat black, water-washable paint to increase the surface conductivity of the test object. After spraying the rack surface with such paint, the thermal variations penetrated to the mid-ply of the

laminate. Although this technique required that the rack panel be inspected from both sides and the rack be sprayed and cleaned up after the inspection, it demonstrated the potential to inspect racks with thermography.

Karabutov et al. (1998) used a laser optoacoustic sensor to nondestructively characterize layered structures of composite materials. Graphite-epoxy composite samples with differing percentages of porosity (<0.1%, 0.4%, and 1.2%) were provided by an aircraft manufacturer. A short laser pulse was used to excite the composite (see Figure 3.2-7). The optical absorption of the material was assumed to be approximately equal to the optical attenuation coefficient. Thermoelastic expansion of the laser-heated layer produces acoustic pressure waves, which propagate into the absorbing and transparent media as ultrasonic pulses. In Figure 3.2-7, The gray area depicts the region of laser-heated material. Small arrows show the direction of particle movement in the material due to thermoelastic expansion. Large arrows indicate the propagation direction for laser-induced ultrasonic pulses in the irradiation geometry that generates planar acoustic waves. In the ultrasonic frequency range form 1 to 5 MHz, the acoustic attenuation coefficient increased with an increase of relative porosity. Also, the "noise" component of the scattered acoustic pulse sharply increased with increased porosity.

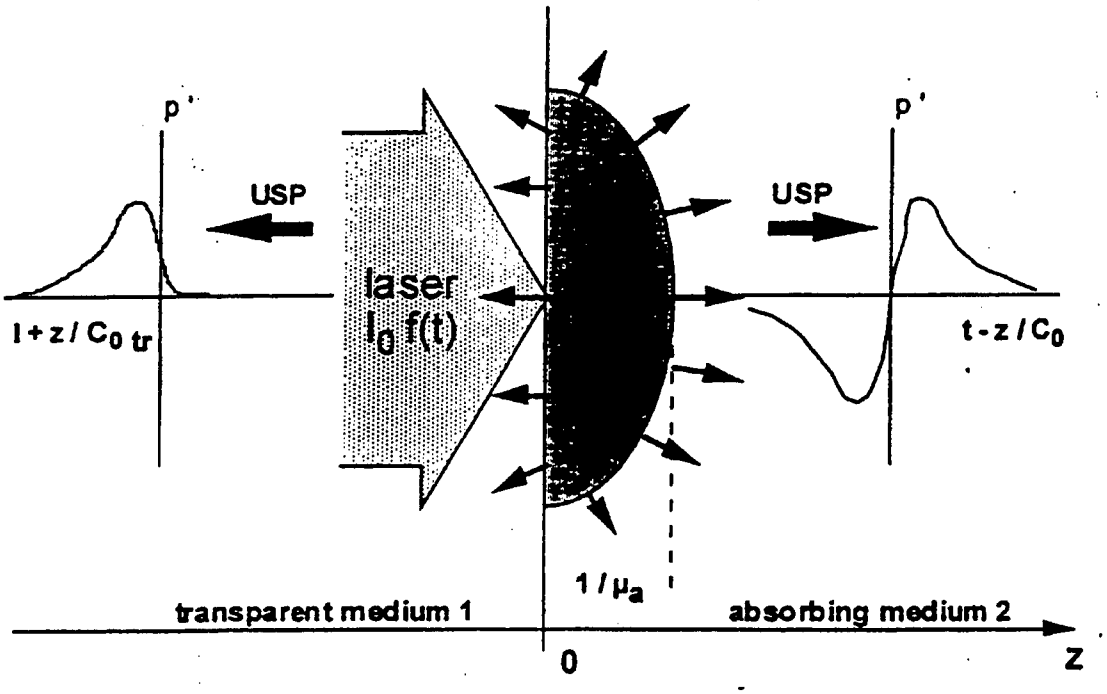

Figure 3.2-7. Schematic of laser optoacoustic evaluation of optically absorbing medium.
(Karabutov et al. 1998)

The author's believed that the spectrum of ultrasonic signals measured with the laser optoacoustic sensor gives a better visual representation of the material's heterogeneous structure. This spectrum consists of two components: a smooth (major) and an irregular (noise-type). The spectral measurement of the noise-type component does not require a reference signal and may be determined independently for each and every sample. Karabutov et al. believe that spectral representation should be used to further analyze laser-induced ultrasonic signals.

Karabutov et al. concluded that laser optoacoustic monitoring might be a method for nondestructive evaluation of the porosity of composite materials, particularly if only one surface is accessible. Furthermore, they believe that a quantitative analysis of the temporal profiles of the backscattered wide-band ultrasonic signals may yield novel quantitative characteristics for graphite composites: a cross section of ultrasound backscattering. A laser optoacoustic sensor was shown to be capable of detecting structural heterogeneities and may potentially reveal the nature of defects, such as porosity or layer separations. And because this technique uses a laser to excite the test object, a couplant is not required, allowing it to be used on in-service structures.

McRae and Zala (1995) characterized the linear variation of attenuation with frequency using the constant-Q model, a model previously developed for use in seismic applications. This method requires only that the acoustic impedances of the system are known and that the surface and interface reflections are resolvable. The accuracy of the method was verified in tests with synthetic data. Values of Q were then estimated for each of a series of six graphite-epoxy laminate specimens with known porosities in the region of 0.34% to 5.33%. These specimens were about 0.29-cm thick and were scanned on a 128-by-128-element grid (2.6 cm on a side); 256-element traces were collected using a broadband 5-MHz focused transducer and sampling rate of 50 MHz. The measurements showed a strong inverse correlation between Q and porosity, and suggest that Q may provide a sensitive and quantitative means of estimating porosity, especially for the critical region of low porosity levels.

3.3 Fiber/Matrix Distribution

The distribution of fibers and matrix is critical to the performance of a composite structure. Knowledge of size and location of matrix-rich pockets and of matrix-starved regions provides important information that can be used in finite element codes to calculate performance influences.

Steiner (1992) used ultrasonic pulse-echo C-scan imaging to evaluate a 64-ply graphite-epoxy specimen. The fiber and matrix components react differently to ultrasonic energy. While the fibers reflect the energy, the matrix tends to absorb some of the energy. These differences may be subtle based on the material system used in the composite, but advanced image enhancement techniques can aid in the determination of matrix-rich or -starved areas in the scanned specimen. Figure 3.3-1 shows the specimen with matrix-rich areas in the center and matrix starved areas on the top.

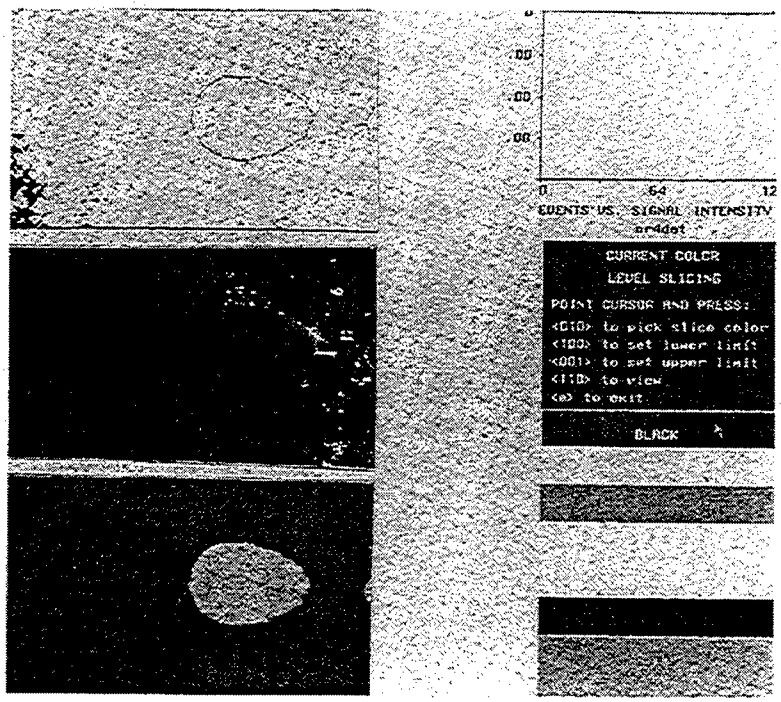

Figure 3.3-1. Unenhanced C-scan of 64-ply graphite-epoxy sample (bottom) with matrix-rich areas (center) and matrix-starved areas (top). (Steiner 1992)

The matrix-rich areas are located on the less-than-average echo intensity side of the pulse-echo histogram, whereas the matrix-starved regions can be found on the higher-than-average intensity side of the histogram. The sample was sectioned to verify the matrix-rich pockets. An analysis of the manufacturing process showed that the autoclave bagging was the primary reason for the variations.

3.4 Fiber Volume Fraction

A composite's strength is determined by the interaction between the fiber and the matrix. Since the matrix distributes the load onto and between the fibers, it is important to know the respective volume amounts to insure proper load distribution.

Many methods exist to experimentally determine the fiber volume fraction (FVF) in graphite-epoxy composites. The most commonly used method of determining composite FVF involves the removal of the matrix by heat (burn off) or chemical (acid) digestion. In addition to being destructive, these techniques are time consuming and require the disposal of toxic wastes.

Zalameda and Winfree (1993) investigated a through-transmission, thermal diffusivity measurement technique to characterize the FVF in graphite composite plates, assuming negligible porosity levels. The samples were 16-ply and 32-ply composite plates with lay-ups of [0/90] 4s and [0/90] 8s. The target fiber volume fractions were 40%, 50%,

60%, 65%, and 70%. Unfortunately, the FVF varied throughout the plates, especially for the higher FVF plates. A single-point diffusivity measurement system was used, with the heat source on one side of the sample and the detector on the other side (see Figure 3.4-1). The detector area was 1 mm in diameter and the measured area (field of view) was approximately 10 mm in diameter. Experiments showed that the higher the heating frequency, the more sensitive the measurement was to diffusivity. It is important to note, however, that the magnitude of the measured temperature oscillation is heavily attenuated as the thermal wave frequency increases. For a known thickness and measured phase, Zalameda and Winfree computed the diffusivity.

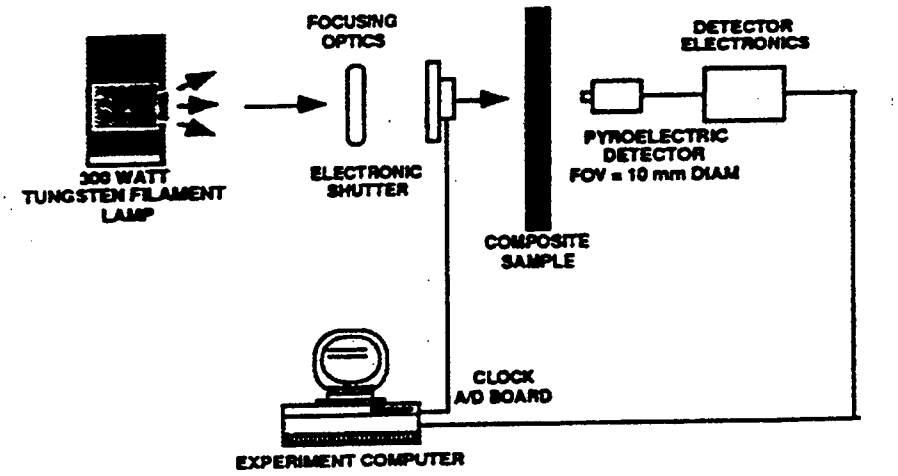

Figure 3.4-1. Single-Point Thermal Diffusivity Measurement Setup (Zalameda and Winfree 1993)

Comparing the predicted diffusivity with the measured diffusivity compared the FVF model with the destructive test results. The thermally measured FVF is typically slightly higher than the destructive test results. This may be the result of the matrix conductivity being slightly higher than the value found in the literature. Also the model did not take into account porosity. The porosity volume fraction would tend to cause the FVF measurement to be increased for the lower FVF and decreased for the higher FVF since the diffusivity value of air is between the matrix and fiber diffusivities. (Zalameda and Winfree 1993)

In 1994 Zalameda and Smith revisited this problem in an effort to develop a nondestructive technique to determine FVF using a dual inspection methodology using the same equipment setup used by Zalameda and Winfree. They described the relationship between thermal diffusivity and fiber, matrix, and void volume fractions in a one-dimensional heat flow model where the void volume fraction is determined ultrasonically. The samples were 16-ply and 32-ply composite plates with lay-ups of [0/90] 4s and [0/90] 8s. The target fiber volume fractions were 40%, 50%, 60%, 65%, and 70%. The thermal properties of the composites were approximated, assuming the heat flow through a plate is perpendicular to the fiber and matrix. Table 3.4-1 shows the model material properties used in the approximations.

Table 3.4-1. Model Material Property Values (Zalameda and Smith 1994)

Property	Fiber	Matrix	Air
Volumetric heat capacity, J/(cm^3-°C)	1.3275	2.162	0.0012
Thermal conductivity, W/(cm-°C)	1.73	0.00173	0.00026
Diffusivity, cm^2/sec	1.24	0.00127	0.2216

Zalameda and Smith's approach to determine the FVF consisted of a single-point diffusivity measurement performed on 1 cm x 1 cm marked areas. To compute an average diffusivity value the heating frequency was varied from 0.3 to 0.8 Hz for the 16-ply samples and 0.1 to 0.35 Hz for the 32-ply samples. At each heating frequency the measurement was repeated seven times. After the measurements were made, the samples were digested with sulfuric acid and 30% hydrogen peroxide. The measurements were then corrected for porosity.

The porosity was determined using three methods: calculating the volume percentage of porosity from the destructive test results; taking photomicrographs of a polished edge where the coupon for the destructive test was removed; and estimating the porosity using ultrasonics wherein the attenuation is assumed to be dominated by scattering. The ultrasonics technique was the only nondestructive method that has field potential. When the slope of the relative attenuation was plotted against the optically determined porosity, a somewhat linear relationship was found with a correlation factor of R=0.58. The porous shapes were nonuniform and this could be one factor contributing to the error. Also within the 10x10 grid, the measured slopes were found to vary widely by as much as 50 percent, thus indicating the nonuniformity of the porosity. However, the relative mean square difference error decreased when porosity values were used to correct the thermally measured FVF values.

3.5 Fiber Orientation

In the flow molding of discontinuous fiber polymer composites, the flow process causes orientation of the fibers in the part. In order to be able to assess the part, it is necessary to know the orientation of the fibers. Flow molding of long-fiber-reinforced molding compounds produces fiber orientations that considerably influence the end properties of the compression-molded parts. Only if the orientations are reliably known is it possible to take full advantage of them and adapt them to the desired requirements.

In addition, in continuous fiber reinforced polymer composites, the fiber orientation needs to be carefully controlled. A part's desired strength can be considerably decreased with just a small variation in the ply orientation. For instance, with a variation of 10 degrees, the stiffness of a composite laminate can be reduced by 30 percent (Sullivan et al. 1996).

De Goeje and Wapenaar (1992) investigated the possibilities and limitations of eddy current methods for inspecting carbon-fiber-reinforced plastic (CFRP) composites. Eddy current methods can only be applied to materials that have high electrical conductivity. In contrast to metals, CFRP composites show inhomogeneous and anisotropic electrical properties (see Table 3.5-1). Moreover, the conductivity is much lower.

Table 3.5-1. Specific Conductivity of Metals and CFRP (de Goeje and Wapenaar 1992)

Material	Conductivity (10^4 S/m)	Direction of Measurement
Copper	5900	
Aluminum	3500	
Iron	1000	
Graphite	13	
Carbon	3	
Carbon fiber	4-17	
Unidirectional	0.9-1.5	Parallel
CFRP	0.01-0.2	Perpendicular
	2	Parallel
	0.01	Perpendicular
	0.13	Parallel
	0.03	Perpendicular
	3.6	Parallel
Satin weave CFRP	0.1-1	

For unidirectional composites the conductivity in the fiber direction is a factor of about 1000 lower than that of metals, while the conductivity in the cross direction is a further factor of about 100 lower. Such reductions require an increase in the measuring frequency by the same factor to observe comparable eddy currents in composites and metals.

The authors tested unidirectional and satin weave carbon fiber/epoxy prepregs. Probes with elliptical coils (shown in Figure 3.5-1) were used to determine the fiber orientation in the samples. The probes were rotated over 360° while the amplitude of the signal induced in the detector coil was monitored. The probe with the two coils aligned did not give a clear picture of the fiber orientation. The measurements show that there is more shielding (lower amplitude) when the long axis of the coils is parallel to the fibers. Even

for the satin weave samples there is a visible angular dependence of the shielding. It appears that the conductivity is still not completely homogeneous in the plane of these samples, despite the "infinite" number of contacts between the fibers.

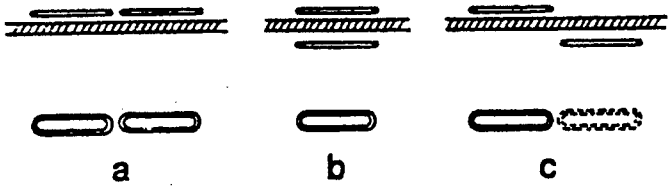

Figure 3.5-1. Schematic representation of the three probes used to detect the fiber orientations in carbon-fiber composites. Each probe consists of a transmitting coil and a receiving coil. (de Goeje and Wapenaar 1992)

A clear picture of the fiber orientation is obtained when the two coils are next to each other. In this configuration the fibers are part of an induction loop formed by the two coils, and the elliptical shape is of minor importance.

De Goeje and Wapenaar explained the inhomogeneities in the unidirectional samples as the strong dependence of the local conductivity on the interlaminar fiber-fiber contacts. The detection of defects in such samples will be hampered by these intrinsic inhomogeneities. The satin weave samples show a more regular response. Because the effect of the interlaminar fiber-fiber contacts on the in-plane conductivity is less for weaves, de Goeje and Wapenaar considered it plausible that the electrical contact between crossing fibers in the weave, which is determined by the lamination pressure and the fiber content, determines the conductivity. They concluded that the variation in the eddy current signal due to intrinsic inhomogeneities of the composites is limited for weaves (about 3%), but can be very large for unidirectional laminates (about 20%).

Mol (1992) developed a method for automatic determination of the fiber orientation by image processing of the ultrasonic C-scan images. This method is based on the observation that fiber orientation is visible in pulse-echo C-scans of individual plies. The samples were made from 6376C/T400H CFRP material, which has a ply thickness of 0.181 mm. Pulse-echo C-scans were made by digitizing each A-scan and by selecting a number of samples with a pre-chosen delay relative to the front surface echo. Fiber orientation was visually detected in the C-scans to a depth of roughly 12 plies. Noise and long wavelength components troubled automatic estimation from two-dimensional Fourier transforms of the images. Local peaks were observed at the wave vector position corresponding to the fiber orientation of most images at the wavelength of the fiber pattern. Fiber orientation estimation from pulse-echo images of individual plies by local contrast stretching and uniform filtering was successful over a depth range of 16 layers in the test material. The determination of the fiber orientation was correct for plies 3 to 16

(0.24 to 2.6 mm deep) and failed one or more times down to ply 22. When measuring deeper than ply 22 the signal-to-noise ratio was too low and all information on fiber orientation was lost.

Schuster and Steiner (1993) attempted to determine fiber direction using a full-waveform ultrasonic backscattering technique on composite specimens with varying fiber directions and different numbers of laminae per direction. Five 16-ply, 60-mm by 60-mm flat plates of epoxy resin and HT carbon fiber with differing fiber directions (0; 0/90/0; 0/+45/-45/90; 0/90/0; and 0/10/45/65) and lay-up sequences were manufactured. Backscattering works by transmitting ultrasonic sound at oblique angles of incidence (see Figure 3.5-2). While travelling through the composite material, the sound interacts with fiber of fiber bundles resulting in a scattered wave back to the transducer. The tests were conducted in an immersion tank with a robotic ultrasonic NDE system.

After performing some initial tests, Schuster and Steiner determined that 15° was the best angle of incidence. They chose the angles of rotation with a small step-size of 5° in directions of existing fiber orientations and larger step-sizes in other directions to reduce the time needed to conduct the tests and to save storage space. After plotting the backscattering results, the fiber direction was easily determined but the number of laminae and the quantitative fiber direction could not be determined. To evaluate the backscattering results quantitatively, the authors developed a special algorithm based on indications that for a 15° angle of incidence, backscattered waveforms can be evaluated similar to regular A-scans. The intensity values were transformed into dB values, followed by the interpolation of relative maximums of the received data per gate as a result of the 5° step width. Based on the interpolated data, the fiber direction for the first gate of sample 2 was evaluated resulting in -5.0° with an intensity of -4.5 dB.

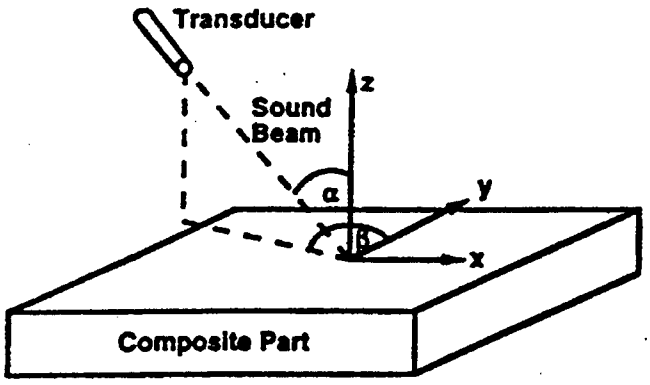

Figure 3.5-2. Basic setup for ultrasonic backscatter testing. (Schuster and Steiner 1993)

Schuster and Steiner also attempted to determine the thickness and number of laminae in a composite sample. The upper laminae were measured with only slight discrepancies that may be explained by the sample not being adjusted correctly in the immersion tank. The difference in the thickness and the number of upper laminae is small in comparison to the error made in deeper sections, which could be explained with different sound velocities parallel and perpendicular to the fibers.

Schuster and Steiner concluded that ultrasonic backscattering was a reliable tool to detect fiber directions and the thickness of layers in the upper regions of composite parts. They determined that further work needs to examine the sound velocity for angles of rotation between 0° and 90° in detail to evaluate deeper sections of parts with the same accuracy as the upper regions.

Backscatter has been successfully applied to map fiber directions, ply gaps, and fiber misalignments by using a polar C-scan system (Sullivan et al. 1996). Without scanning, the fiber directions can be locally determined by simply rotating the laminate using the backscatter technique. For laminates having many fiber directions, this can become extremely time consuming. Although this technique is a useful tool, a correlation between the lay-up sequence and the backscatter data has not yet been satisfactorily established. An optical technique has been investigated that utilizes optical backscatter from the fibers using a probe that is inserted into a hole drilled through the composite. Even though this is a reliable method for ensuring correct lay-up sequence, this technique is extremely localized (will not be useful to evaluate fiber waviness or regions of fiber misorientation) and requires drilling a hole, which is not usually feasible in actual structures.

Sullivan et al. (1996) conducted an experiment to study ultrasonic plate wave (also called Lamb wave) flow patterns in anisotropic and multi-layered composite materials. Fiberite HYe 1034C prepreg unidirectional tape was used to fabricate all test specimens. All but three of the specimens were 20 plies thick. In the test setup, one transducer transmitted the ultrasonic wave into the specimen while the receiving transducer captures the leaky plate waves that emanate from the top surface of the laminate (see Figure 3.5-3). The transmitter was fixed such that the transmitting probe insonified the test piece at one end, while the receiving transducer scanned the laminate. Both transducers were maintained at the same height from the laminates, and a 10° angle of incidence was used for both transducers. Plate waves were generated to image the flow patterns of ultrasonic waves in multiple laminates of various fiber directions.

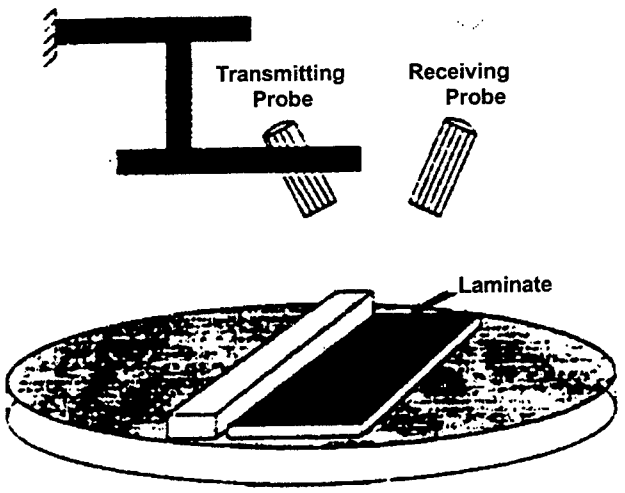

Figure 3.5-3. Setup for plate wave flow pattern method. (Sullivan et al. 1996)

The results showed that the waves propagate long distances along the fibers when compared with 90° (perpendicular) to fiber direction. Also, the beam spreading was more noticeable when the plate waves propagated across the fiber. Sullivan et al., demonstrated that the coupling between the inner and outer plies do not significantly affect the flow patterns even when more than one ply orientation exists in a laminated structure. The energy propagates along all fiber directions even in cases of specimens with fibers in many directions.

Since the fiber directions of the laminates had been successfully mapped, Sullivan et al. decided to investigate the response to different frequencies. A frequency analysis was conducted based on the principle that there are several modes that are simultaneously generated, and each mode has a unique displacement and stress profile across the thickness of the laminate. Hence, if individual modes are isolated, especially ones that have concentrated displacement/stress values across specific ply groups, and knowing the mode shape of the displacement/stress, individual ply groups can be located. This portion of the study established that selective imaging of individual ply orientations using narrowband frequency analysis is possible, and depending on the desired depth, appropriate plate wave modes can be generated.

Sullivan et al. showed that the plate wave flow pattern technique was successful in mapping the fiber directions of a multi-ply laminate. They also developed a frequency-based analysis method to analyze the experimental plate wave flow pattern data. Using the frequency filtering method, they showed that the potential for a ply-by-ply fiber orientation analysis exists, if suitable parameters are selected. This technique can be used either as a local method or as a global scanning technique.

Most recently, Michaeli et al. (1999) used X-rays and image processing to determine fiber orientation of long-fiber-reinforced molding compounds in compression-molded parts. After a part was imaged, the X-ray was digitized and transferred to a personal computer for analysis. First, edge extraction was performed with the aid of differential operators. A gradient of gray-scale values exists between the fibers (bright areas in the X-ray) and the matrix (dark areas) that were used to detect the edge and thus the outline of the fibers. The edges of a fiber are characterized by high gray-scale gradients. For every pixel, the Sobel operator (calculates the difference between a given value and its next-but-one neighbor) was used to calculate the gray-scale gradients in the X and Y axes. The edges were detected by means of a defined threshold value. Only if the gray-scale gradient of a pixel exceeds the threshold value is an edge indicated. If the system determined that a pixel was lying on an edge, the direction of this edge and the orientation of the fibers were calculated. The number of detected orientations was counted for each angle between 1° and 180° and written as a histogram into a results file. The last stage in the x-ray image analysis consisted of calculating the fiber distribution function. Michaeli et al. concluded that the experimental and theoretical results showed that the X-ray and image processing system for measuring fiber orientation was sufficiently accurate and was suitable for verifying simulation results. Moreover, the system has proved to be an important quality assurance tool for several companies.

3.6 Fiber Waviness

Fiber waviness can be viewed as the through-thickness undulation of fibers in a thick section composite, and is a manufacturing defect that is often introduced during manufacture. Fiber waviness can occur during the filament winding process when wet hoop-wound filaments are under stress from the over wrapped layers, or from the buckling of prepreg. In addition, it can occur during the cure cycle as a result of residual stress build up. Since fiber waviness can cause a significant reduction in strength and stiffness of the final product, nondestructive evaluation techniques are needed to detect and quantify this defect.

Wooh and Daniel (1994) studied the application of ultrasonics to characterize the fiber waviness in thick composites. The authors used elastodynamic ray theory to develop an ultrasonic method for detection and characterization of fiber waviness in thick section composites. The authors studied a series of filament wound carbon/epoxy composites and measured the amplitude (0.1 in.) and period (1.2 in.) of the waviness optically on machined surfaces of the cross section of the samples. In addition, a reference sample was prepared with virtually no waviness.

The authors reported that they were unsuccessful in using conventional C- scanning or quantitative measurements to characterize the fiber waviness. This was due to the refraction of the propagating ultrasonic beam. To over come this difficulty the authors used ray-tracing techniques. Figure 3.6-1 shows the ray tracing maps generated for a wavy layer composite.

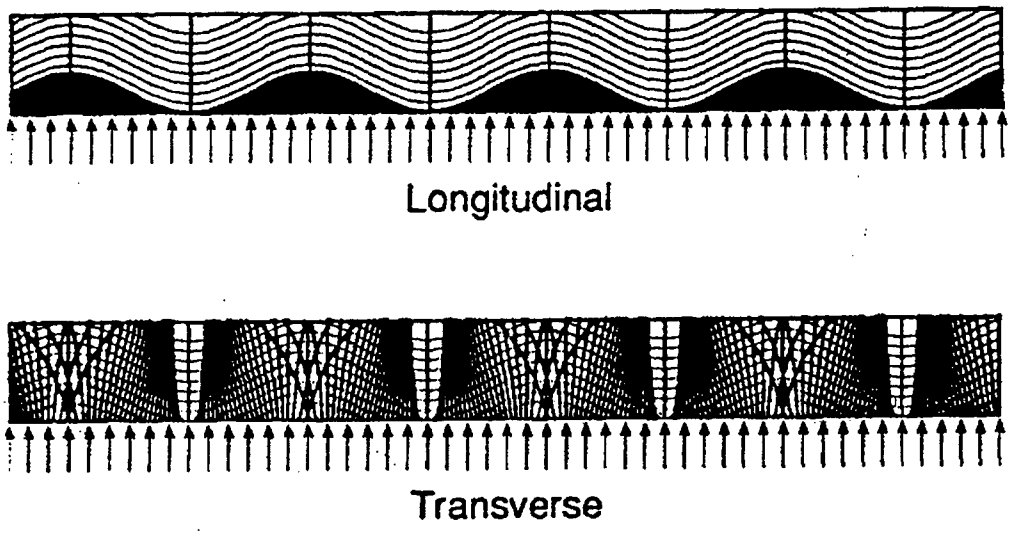

Figure 3.6-1. Trace maps of rays in 200-ply IM6G/3501-6 unidirectional lamina with wavy fibers.
(Wooh and Daniel 1994)

Wooh and Daniel were able to validate these ray trace maps by experiments on the composite samples. However they were only able to obtain qualitative and not quantitative verification of the comparison of the optical results to the ultrasonic experimental results.

Recently, Chun and Jang (2000) investigated, both experimentally and theoretically, the use of conventional ultrasonics to determine uniform fiber waviness in thick section composites. The authors studied a series of specially fabricated thick section graphite/epoxy composites with varying degrees of fiber waviness. There were three different degrees of fiber waviness that had fiber waviness ratios of 0.011, 0.034, and 0.059 where the fiber waviness ration is the ratio of the amplitude of fiber waviness to the wavelength of fiber waviness.

The authors used 10MHz center frequency transducers in a through-transmission mode and measured time of flight and total energy received at different positions on the samples. The authors concluded from their numerical simulations and experimental data that the wavelength of the fiber waviness can be determined quantitatively by the relative distance between the peaks during scanning. In addition, they concluded that they could qualitatively determine the degree of fiber waviness by utilizing changes in the ultrasonic wave travel time.

Joyce et al. (1997) extensively reviewed the literature for NDE techniques to determine fiber waviness in composites. They came to the conclusion that due to the complicated nature of acoustic waves propagation in wavy composites, the challenging problem of

characterizing natural fiber waviness using ultrasonics remains largely unsolved. They also reviewed conventional x-ray radiography and concluded that some success was demonstrated using embedded tracer fibers that have a higher contrast to x-rays than the conventional fibers and polymer matrix. Tracer fibers of leaded-glass were successfully used with conventional radiography, and large boron fibers were easily seen in with optical inspection.

Joyce et al. also speculated on the application of computed x-ray tomography for determining fiber waviness and believed that it might be useful. They also speculated on the use of eddy current measurements to determine fiber waviness in carbon fiber composites and did not reach a conclusion.

The authors then reviewed the literature on the use of optical microscopy to determine fiber waviness is carbon fiber composites and concluded that optical microscopy is the most powerful NDE tool currently available for determining fiber waviness in carbon fiber epoxy composites. Joyce et al. then experimentally developed and demonstrated an optical microscopy technique for determining the waviness in carbon/epoxy composite. They used an inverted metallograph at 80x magnification and dark field illumination to determine the amplitude and wave length of the wrinkled regions.

They concluded that since most of the process induced fiber waviness in unidirectional thermoplastic laminates is clearly discretized into little fiber–wrinkled regions, the spatial distribution of fiber waviness can be estimated from surface inspection of the laminates by optical microscopy. However, it should be stressed that this technique is operator dependent and also needs to be coupled with highly destructive and time-consuming sectioning of the composites to truly determine interior fiber waviness and any in-plane/out-of-plane character of the waviness. It therefore appears that this laboratory technique based on optically microscopy is severely limited for any use in manufacturing application.

To overcome the difficulties that are inherent in using 2D optical microscopy to determine fiber waviness in composite, Clark et al. (1995) developed a novel 3D optical method for determining fiber waviness in composites. They utilized a confocal laser-scanning microscope which appears to be a very powerful technique for use in the laboratory to study and characterize fiber waviness on highly polished samples. However, it appears that the technique has severe limitations for use in manufacturing.

In summary, the methodology to determine fiber waviness is limited to destructive analysis using optical microscopy. All of the NDE techniques based on ultrasonics, eddy currents or X-ray radiography should be viewed as works in progress, and they all currently have severe limitations in obtaining quantitative information.

3.7 Delaminations

Fiber reinforced polymer matrix composites are widely used in many industries for applications that require critical structural components. In most of these applications delamination between the fiber plies is one of the most serious type of flaws that can occur in these components. Delamination can occur when contaminated pre preg is used during lay up, and during use as a result of impact damage, fatigue or erosion. Delamination can affect the structural integrity of the composite by reducing the compressive strength and the mechanical stiffness. In addition, structural integrity can be severely compromised by delaminations that cause a reduction of material thickness attached to a sub-structure. Delamination is sometimes referred to as a crack-like discontinuity between plies and may propagate during use due to mechanical or thermal loads. In the worse case, a delamination may propagate and cause fracture of the material. Therefore, the nondestructive evaluation of delaminations is very important in both the manufacture and in service sustainment of these materials.

A number of NDE techniques have been widely used to detect delaminations. Techniques that are well established include visual inspection, tap testing, resonance methods, ultrasonic testing, thermography, eddy current testing, and x-ray radiography. However, inspection of composites is a difficult task due to their multi-layered structure, anisotropy and heterogeneity and inspection with current techniques can still be a difficult task. Newer techniques such as shearography have shown great promise and have found widespread use, but shearography is relatively costly and therefore not likely to meet all needs. Therefore, research and development to improve the usefulness and capability of NDE for detecting and characterizing delaminations is continuing.

Gros (2000) reviewed the current and future trends in the nondestructive testing of composite materials for a variety of defects including delamination. The author discussed visual examination, electromagnetic testing, infrared thermography, acoustic techniques and radiography. Gros concluded that ultrasonics and thermography will benefit from further improvements, and electromagnetic techniques will find increasing use due to their relatively low cost. In addition, the author speculates that self-diagnostic composite materials may see an increase in use. These self-diagnostic materials could contain optical or electrically conducting fibers that would permit monitoring of changes in optical or electrical properties of the fibers as the materials are subjected to stress and strain. Gros also expects that multi sensor systems will find more widespread use and require enhanced data fusion capabilities.

During the last five years, several researchers have studied ultrasonic methodology to enhance capability to detect and characterize delaminations in composites. Scarponi, and Briotti (2000) developed a novel ultrasonic inspection method for evaluating delaminations in carbon-fiber, glass-fiber, and Kevlar-fiber reinforced plastic composite materials. The NDE system the authors used operated in the 5 to 15 MHz range and provided for measuring the maximum ultrasonic echo amplitude. This capability coupled with mapping soft and hardware allowed the exact location and extent of a delamination to be determined because of the relationship between the damage extent and the echo

amplitude. In addition, the ultrasonic system could be operated in a relative depth mode where the ultrasonic echo delay is measured. The delay time is used to determine the relative depth of the delamination in terms of a percentage of the specimen thickness.

The authors concluded that their ultrasonic technique has good capability to detect, locate and evaluate delaminations in a wide variety of fiber-reinforced composite materials. However, the authors caution that the technique requires the proper selection of probe frequency, and they recommend that extreme care must be taken in instrument calibration and use. In addition, a high level of operator skill is required to obtain reliable results.

Recent work by Mouritz et al. (2000) studied the use of low frequency pulse-echo ultrasonics for detection of fatigue damage in thick section composites used in maritime vessels such as yachts, lifeboats, fishing trawlers, patrol boats and naval mine hunting ships. Ships made of glass reinforced polymer composites are expected to operated for 20-50 years with out any major structural retrofit. As a result their endurance and safety are dependent on the long-term fatigue performance of the glass reinforced polymer composite. Although the fatigue resistance of glass reinforced composites used in ships is generally good, fatigue damage can develop in highly stressed regions by the repeated action of waves slamming into the hull, and by the hogging-sagging bending motion along the vessel in heavy seas.

Since this type of fatigue damage, which includes debonding of the surface glass fiber tows along with a complex array of cracks and delaminations within the structure is not visibly detected in the early stages, regular NDE of the ships are needed. A wide range of NDE techniques can be used to detect damage in glass composites including tap testing, mechanical impedance thermography, laser shearography, and x-ray radiography. However very few techniques are suitable for inspecting ships at sea, or in a dockyard. A number of factors contribute to the popularity of pulse-echo ultrasonics for this type of inspection including safety, reliability, capability to measure with access to only one side, and portability of instrumentation. However, the delaminations and cracks that grow with low-level fatigue are difficult to detect with ultrasonics since they grow parallel to the transmission direction of the ultrasonic waves. Mouritz et al. used the experimental arrangement shown in Figure 3.7-1 to study delaminations in thick composites.

Although the authors used this technique to study fatigue damage in the laboratory, they concluded that the technique would not be suitable for inspecting ships with low fatigue stress damage in ships. This was the case because of the large variation in attenuation in the thick glass composites. Figure 3.7-2 shows the type of low stress fatigue cracking studied by the authors. On the other hand, the authors concluded that high fatigue stress damage in ships may possibly be detected with pulse-echo ultrasonics since the damage is confined to the surface tows.

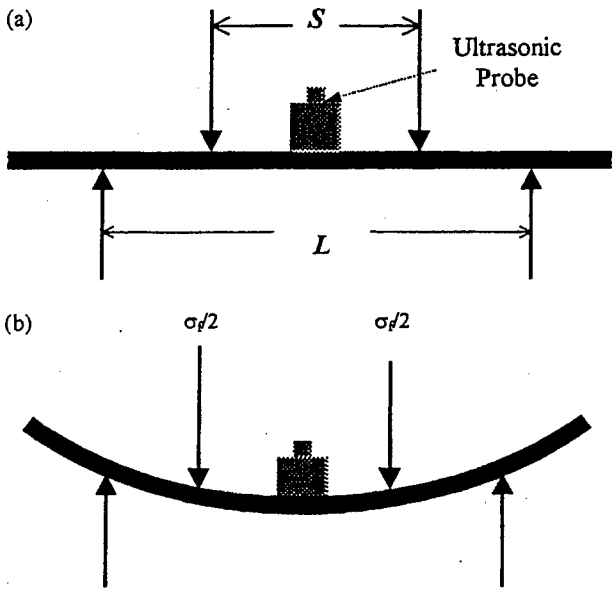

Figure 3.7-1. Experimental arrangement for the four-point flexural fatigue test when the specimen was ultrasonically inspected in the (a) unloaded and (b) loaded states.
(Mouritz et al. 2000)

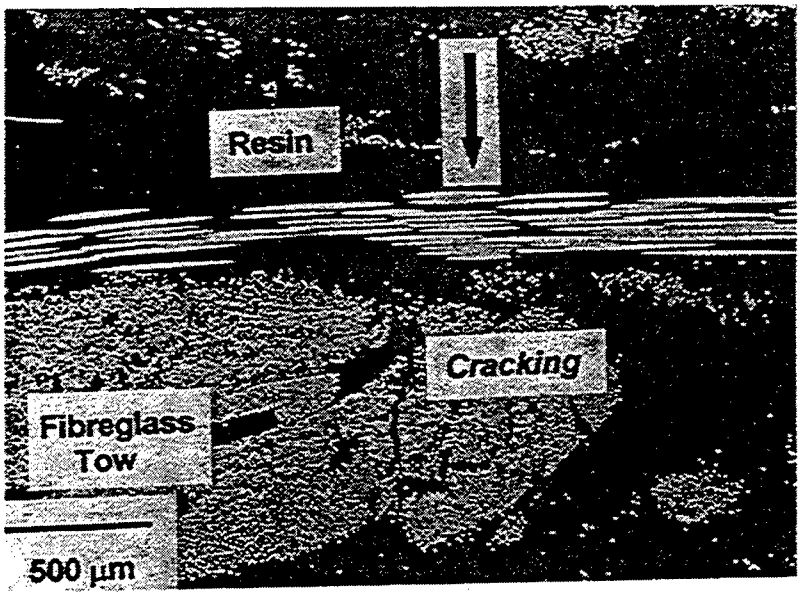

Figure 3.7-2. Low-stress fatigue cracking in a glass reinforced plastic composite tested at a low normalized fatigue stress (σ_f/σ_0=0.36) for 20,000 cycles. The arrow shows the transmission direction of the ultrasound waves.
(Mouritz et al. 2000)

Smith et al. (2000) studied the use of ultrasonic pulse echo amplitude to size delaminations in fiber-reinforced composites. The authors studied the simple amplitude method within the near field of a transducer for sizing delaminations where small defects are sized by measuring the amplitude of the signal reflected from the defect. A theoretical treatment of the measurement was verified experimentally with delaminations of known sizes. The authors used a standard reference panel, shown in Figure 3.7-3, in their experimental studies. In this Figure, the top three rows of defects are fabricated using two layers of 50 μm-thick PTFE sealed around the edges with heat-resistant tape, whilst the other defects are single layers of 50 μm-thick release film. Nominal widths and diameters of the inserts are 25, 12 and 6 mm.

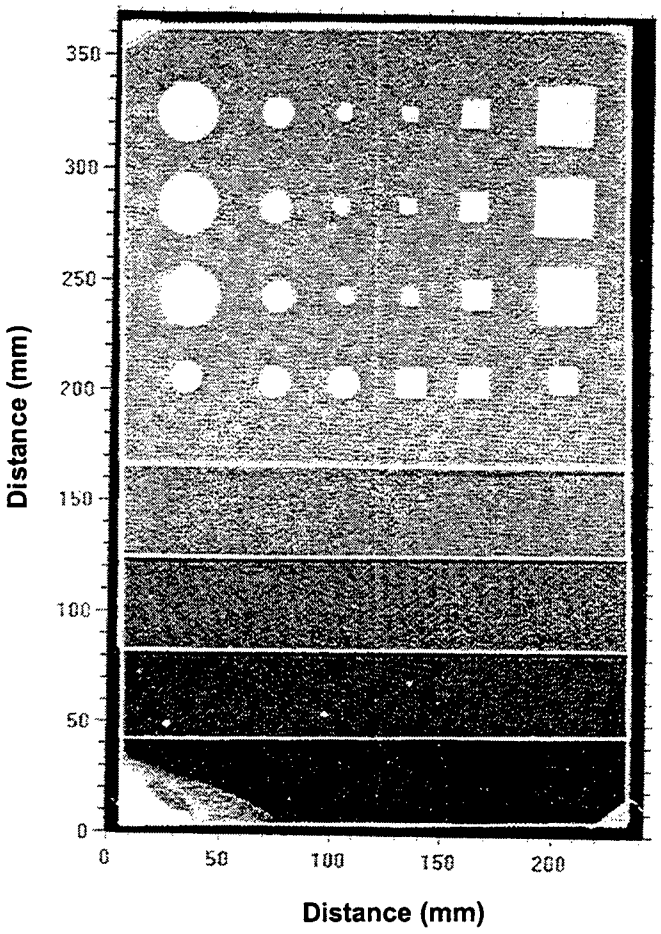

Figure 3.7-3. Double through-transmission scan of the NPL-designed standard reference panel with 24 reference defects and stepped thicknesses of 5, 4, 3, 2 and 1 mm. (Smith et al. 1997)

Despite verifying the theoretical treatment experimentally, the authors believe that the amplitude method is not to be recommended for delamination sizing in fiber-reinforced composites because of the large uncertainty levels in the results. The authors conclude from their study that errors of 20 % in defect area were caused by an error of only 1.85 dB in the refection coefficient of a delamination. In addition, the inhomogeneous nature of composites and the variable reflection coefficients of defects have resulted in random errors of plus or minus 40% in the estimated defect area.

Hesiehurst et al. (1998) applied a new portable holographic interferometry testing system to determine the location and direction of growth of delaminations in composite panels. Figure 3.7-4 shows the holographic interferometry system layout used by the authors.

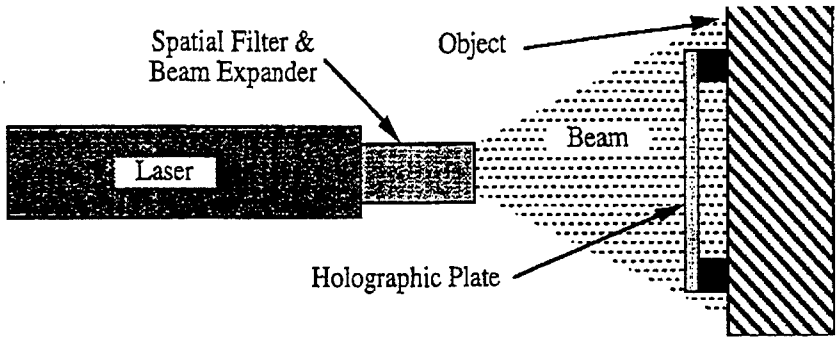

Figure 3.7-4. Holographic interferometry system layout. (Hesiehurst et al. 1998)

Holographic interferometry can be used to determine the contour shapes of the out-of-plane displacements of a surface. Hesiehurst et al. (1998) used reflective holographic interferometry, which is an optical method that produces an interferometric fringe pattern superimposed on the region of interest. The fringe lines represent points or lines of equal out-of plane displacements. The horizontal distance between each fringe represents a vertical distance equal to half the wavelength of the emitted laser light (on the order of 0.6328 micrometers when using a helium-neon laser). The procedure for producing a holographic interferogram is relatively straightforward: 1) a holographic plate is attached to the region of interest, 2) after applying an initial load, the holographic plate is exposed to the laser light, 3) the load is marginally increased and the plate is exposed for a second time, 4) the holographic plate is then developed, and 5) the developed holographic plate is then viewed using reflected white light.

Hesiehurst et al. used this methodology to study delamination of composites under compressive load. and concluded that this holographic technology can be use to determine the location of the site with maximum out-of-plane gradient of the delamination buckle. When viewing a hologram, this site is the likely spot for delamination propagation. They also concluded that the characteristic shape of the delamination buckle would indicate the direction of delamination growth. Although the

authors used this technique in a laboratory study to enhance the understanding of the delamination process, they speculate that it is also applicable to determining the severity of delamination in composite structures.

Several authors have used electrical measurements to characterize delaminations in carbon fiber composites. Todoroki et al.(1995) used the electric potential method to detect delaminations. The authors used the electric bridge circuit approach to determine changes in electrical resistance as a function of delamination or crack length. The authors conclude that this type of NDE measurement is excellent for detecting delaminations in aircraft structures. This technique only requires low currents so the composite structure is not heated. However, electrodes must be attached to the composite for inspection.

In a similar study, Wang and Chung (1997) used electrical resistance measurements with four point probe instrumentation to sense delaminations in carbon fiber composites. The authors concluded that the sensing of delaminations in a cross ply (0/90) continuous carbon fiber polymer composite during fatigue was demonstrated in real time by electrical resistance measurements in the through thickness direction. Figure 3.7-5 shows the variation in resistance, $\Delta R/R_0$ as a function of % fatigue life.

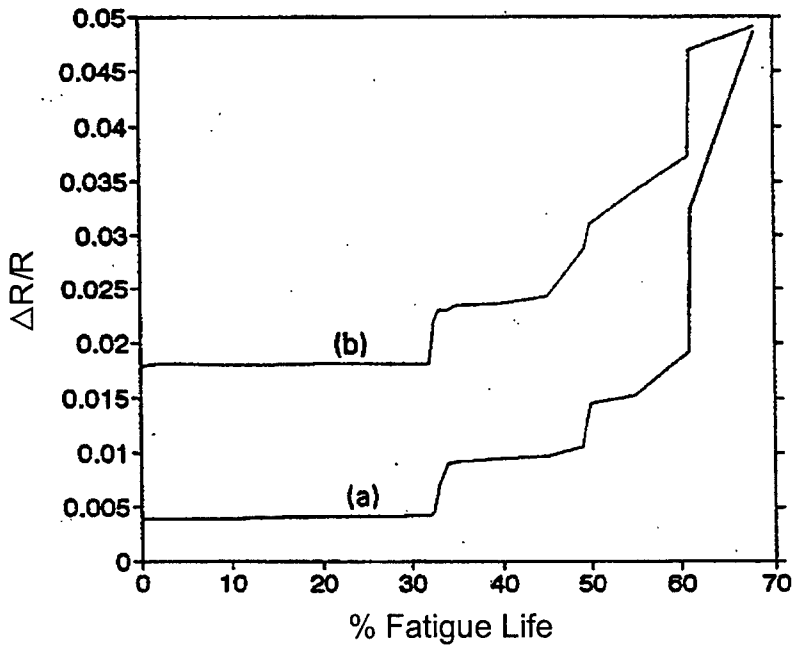

Figure 3.7-5. Variation of $\Delta R/R_0$ in the through-thickness direction with the percentage of fatigue life during tension-tension fatigue for a crossply composite. (a) Minimum $\Delta R/R_0$ at the end of a cycle. (b) Peak $\Delta R/R_0$ in the middle of a cycle.
(Wang and Chung 1997)

Gros and Takahashi (2000) have investigated the use of Foucault currents, commonly referred to as eddy currents, to detect and quantify delaminations in carbon fiber polymer composites. The authors made note of the fact that at the 1993 European meeting of the Annual Congress of Civil Aviation plans were developed for an R&D program on eddy current NDE for assessing the integrity of carbon fiber polymer composites. Partly as a result of these plans, research interest has started and is growing on electric and electromagnetic methods for inspecting carbon fiber polymer composites.

The authors used a commercial eddy current instrument with a high frequency (2 MHz) and a small probe diameter (2 mm) with manual scanning in their experiments. They characterized delaminations in a 24-mm by 14-cm by 1.14-mm thick specimen. The frequency can be selected to control the depth of penetration of the eddy currents. The specimens were quasi-isotropic laminates with a layer arrangement of (0/ -45 /+45 / 90 degree) and had real delaminations introduced by tensile load. The delaminations apparently were characterized by optical microscopy at the edges of the sample and these results were compared to the eddy current results. The authors concluded that eddy current testing is a potential method for the nondestructive detection and characterization of delaminated area at interfaces between plies in carbon fiber/epoxy laminates.

A number of researchers have investigated the feasibility of embedding optical fibers into composites for the purpose of health monitoring of composite structures for delaminations. Sirkis et al.(1994) investigated the effects of embedding optical fibers in graphite/epoxy laminated composite panels. They embedded optical fibers ranging in size from 80 to 600 micrometers at the laminate mid-plane. They then subjected the panels to low velocity impact damage to induce delaminations. With the exception of the 600 micrometer optical fibers, they found that the optical fiber sensors embedded in the mid-plane of the laminates did not influence the size or distribution of the delamination damage. The authors used x-ray radiography, ultrasonic C-scans, and volume visualization to determine if the embedded sensors influenced the macroscale delamination damage in composites.

Elvin and Leung (1997) carried out a theoretical study of the feasibility of using embedded fiber optic sensors to monitor for delaminations in composites. The authors used a physically modeling of the measurement method approach to reach their conclusions. As a result of their modeling efforts, they conclude that the very small incremental changes in the length of embedded optical fibers can be used to determine the size and location of delaminations in fiber composites.

Park et al. (2000) studied the use of embedded extrinsic Fabry-Perot interferometer optical fiber sensors to detect delamination and buckling in composites. Figure 3.7-6 is a schematic of the fiber optic sensor constructed by the authors. These sensors had a diameter of about 250 micrometers and were constructed using single mode and multi mode fiber that were connected together by using a quartz capillary and epoxy. The space between the ends of the fibers was controlled to give Fresnel reflection (about 10 to 50 micrometers). The sensors were embedded in graphite/epoxy laminates that were then

subjected to compression tests. The authors concluded that the compression tests of the composite beams with the embedded fiber optic interferometer were successful. They also concluded that these sensors are a powerful tool that can be used to identify the onset of buckling and delamination in composites.

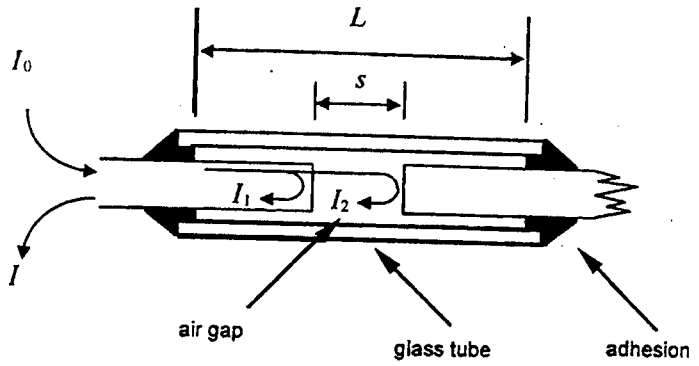

Figure 3.7-6. Schematic diagram of fiber optic sensor. (Park et al. 2000)

3.8 Impact Damage

Nondestructive detection and characterization of impact damage is an important issue in utilization of fiber reinforced composites. For example, it is not uncommon for composite structures to exhibit invisible front surface damage from foreign object impact but have extensive back surface damage. Indeed with the increasing use of fiber reinforced composites for primary an secondary aircraft structures, a major concern for the designer is the knowledge of the effect of impact damage on the residual structural performance of these materials. The ability to characterize nondestructively the impact damage and predict the residual strength of the damaged structure is of major importance for an effective damage tolerant design and provides also tools for in service supportability. Gottesman and Girshovich (1998) have reported development of an analytical damage model for thick laminates loaded in compression. The mechanical damage model was based on damage assessment evaluations provided by ultrasonics and a destructive x-ray microfocus technique combined with an opaque penetrant for damage enhancement. Using the mechanical damage model, a failure model was constructed that led to failure prediction. The analytical models were successfully verified experimentally for various materials impacted at different energies. Gottesman and Girshovich suggest that the combination of nondestructive damage characterization and analytical modeling enables the evaluation of the degradation of the mechanical behavior of impacted composites laminates.

Earlier work by Zalameda et al. (1994) demonstrated that a multi-disciplinary approach for impact damage detection in composite structures can provide a reasonably efficient inspection. In this work, a thermal inspection technique was used to rapidly identify the

impact damage and ultrasonic volumetric imaging quantified the impact-generated delaminations through the volume of the structure. In more recent work by Ball and Almond (1998) the possibility was explored of using transient thermography along with image analysis approaches to detect impact damage in thicker composites. Carbon fiber reinforced plastic (CFRP) laminates ranging in thickness from 3.44 mm to 13.76 mm were investigated. Laminates damaged by low velocity impact were examined with transient thermography and a commercial image processing package and the results compared with ultrasonic c-scans and sectioning. The thermography images demonstrated the ability of the technique to detect the presence of impact damage in all of the specimens examined. Damage area estimates from front face thermographic images correlated with measurements of sub-surface damage obtained from sectioned samples but did not correlate with the c-scan results. Damage areas produced by back face thermographic images correlated well with those obtained from sectioned specimens as well as with C-scans for thinner specimens but not for the thicker (13.76 mm) specimens. Based on plots of thermographic damage area vs. C-scan damage area Ball and Almond suggest that a minimum threshold damage size exists which is not detectable by transient thermography using the equipment and methods applied in their work.

In further development of thermographic inspection approaches for composites, a recent report by Bai and Wong (2001) discusses the use of lock-in thermography. Lock-in thermography utilizes an infrared camera to detect the surface temperature of a thermal wave propagating into the material and then produces a thermal image, which displays the local variation of the thermal wave in phase or amplitude. Defects are detected by differences in phase or amplitude between defective areas and non-defective areas. As in most nondestructive inspections, parameters should be optimized to maximize the difference between defective areas and non-defective areas. The phase difference depends on the thermal properties of the material, the subsurface structure of the sample, the modulation frequency and the surface heat transfer coefficient. Also, in real applications, such as inspection of aircraft structures, the effect of surface convection caused by airflow in natural ambient environments can be significant for some thin structures in which the dominant mode of heat transfer is convection. In order to better understand the behavior of thermal waves under these conditions, Bai and Wong developed a photothermal model for lock-in thermographic evaluation under convective conditions of CFRP plates of finite thickness in which defects were implanted. Experiments were performed to verify the photothermal model and determine the detectivity of lock-in thermographic inspection of the plates. The CFRP specimens were 300 mm x 300 mm x 4.2 mm thick. Artificial defects comprising Teflon films 0.2 mm thick were implanted in the specimens. Defects with diameters ranging from 1 mm to 11 mm were inserted at depths ranging from 0.28 mm to 2.8 mm. A comparison of experimental results obtained from the 11-mm diameter defect at a depth of 0.56 mm and the theoretical results obtained with the photothermal model are shown in Figure 3.8-1.

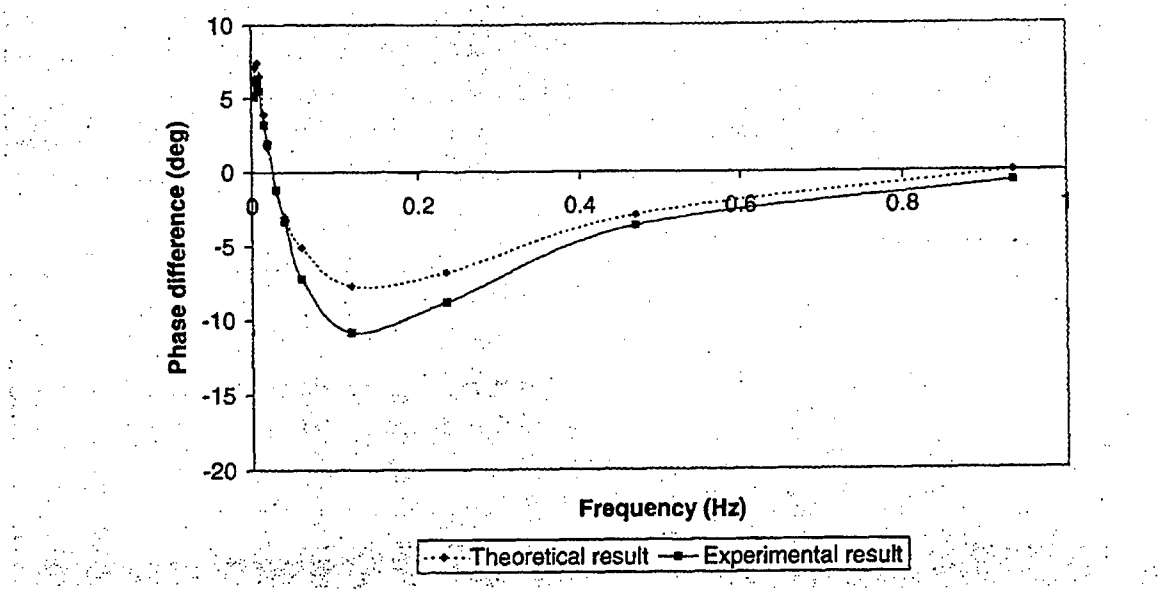

Figure 3.8-1. Experimental and theoretical phase differences between defective areas and non-defective areas produced by a 11-mm diameter defect at a depth of 0.56 mm.
(Bai and Wong 2001)

In this Figure, the phase differences between the central point of a defect image and the average phase value of its surrounding were calculated as the experimental result. As can be seen, although the theoretical and experimental results have similar trends, the phase differences obtained experimentally are larger than those obtained theoretically; this was the case for all defect depths. Bai and Wong attribute this discrepancy to ignoring thermal contact resistances between interfaces owing to the difficulty in determining these numbers. This would be expected to lead to more conservative predictions. From Bai and Wong found that there are frequencies for a specific defect at a certain depth where the phase difference produced by the defect is very small, or zero, and other frequencies where maximum positive and negative phase differences are produced. Also the optimum frequencies change with depth and the deeper the defect the lower the optimum inspection frequency. Since, the optimal frequencies obtained theoretically are very close to those obtained experimentally, the photothermal model can be used to predict optimum inspection frequencies and is useful for selection of inspection parameters.

Another approach to non-contact, whole-field, real-time characterization of impact damage in composite materials is electronic speckle pattern interferometry (ESPI) (Richardson et al. 1998). ESPI is one of a family of coherent light interferometry techniques that also include holographic interferometry, speckle interferometry and speckle shearography. Each is capable of measuring either surface displacement or displacement derivatives with practical benefits of being able to make whole-field, non-contact measurements. ESPI has potential for detection of defects in composite materials due to its advantages of real-time measurement, electronic output as well as the direct indication of defect features. Richardson et al. investigated the applicability of using

ESPI intensity fringes and phase maps to evaluate internal damage in glass fiber reinforced polyester composite materials. An illustration of their experimental setup is shown in Figure 3.8-2.

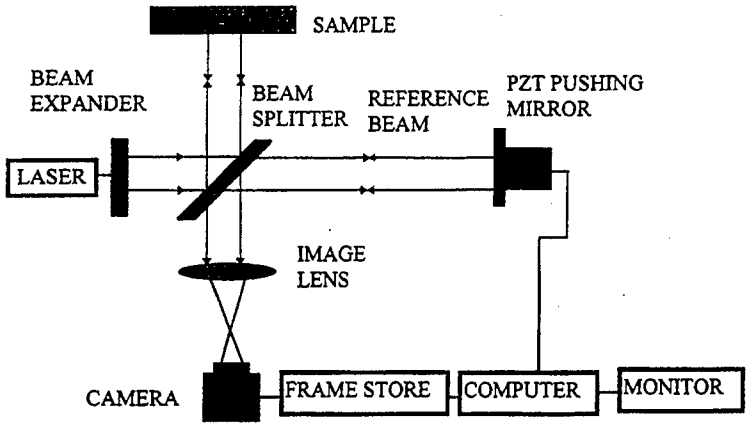

Figure 3.8-2. Optical configuration of phase stepping ESPI. (Richardson et al. 1998)

Phase maps were produced in parallel with intensity fringes to show damage features as well as to indicate the difference between intensity fringes and phase maps in terms of visibility and readability. Both the intensity fringes and the phase maps show the existence of internal damage. The dynamic variation of intensity fringe patterns associated with defects can be readily monitored in real time. Unfortunately, they are not always of good visibility because the spatial frequency distribution of a speckle pattern containing the data signal is embedded in noise. Another problem is the interference of rigid-body-movement-induced background fringes not associated with the damage. On the other hand, fine details of damage can be easily visualized using phase maps with very high visibility and readability as shown in Figure 3.8-3. Damage areas in the specimens were verified using ultrasonic C-scan and sectioning. Test results from an ultrasonic C-scan are shown in Figure 3.8-4 and damage profiles determined using sectioning are shown in Figure 3.8-5. These test results bear close geometrical resemblance to both the intensity fringes and phase maps from ESPI (see Figure 3.8-3); however, there are notable differences in terms of calculate damage areas as shown numerically in Table 3.8-1.

Although phase maps can be directly linked with damage and are straightforward to interpret, real-time observation cannot be achieved due to intensive post-processing computation. Richardson, et al point out that in the broader scientific sense, in the case of phase mapping there is the potential to extract information from the computer that which could quantify the level of damage and which could be used to alert, say a quality control operator, to the need to make further decisions thus providing an automated nondestructive inspection approach.

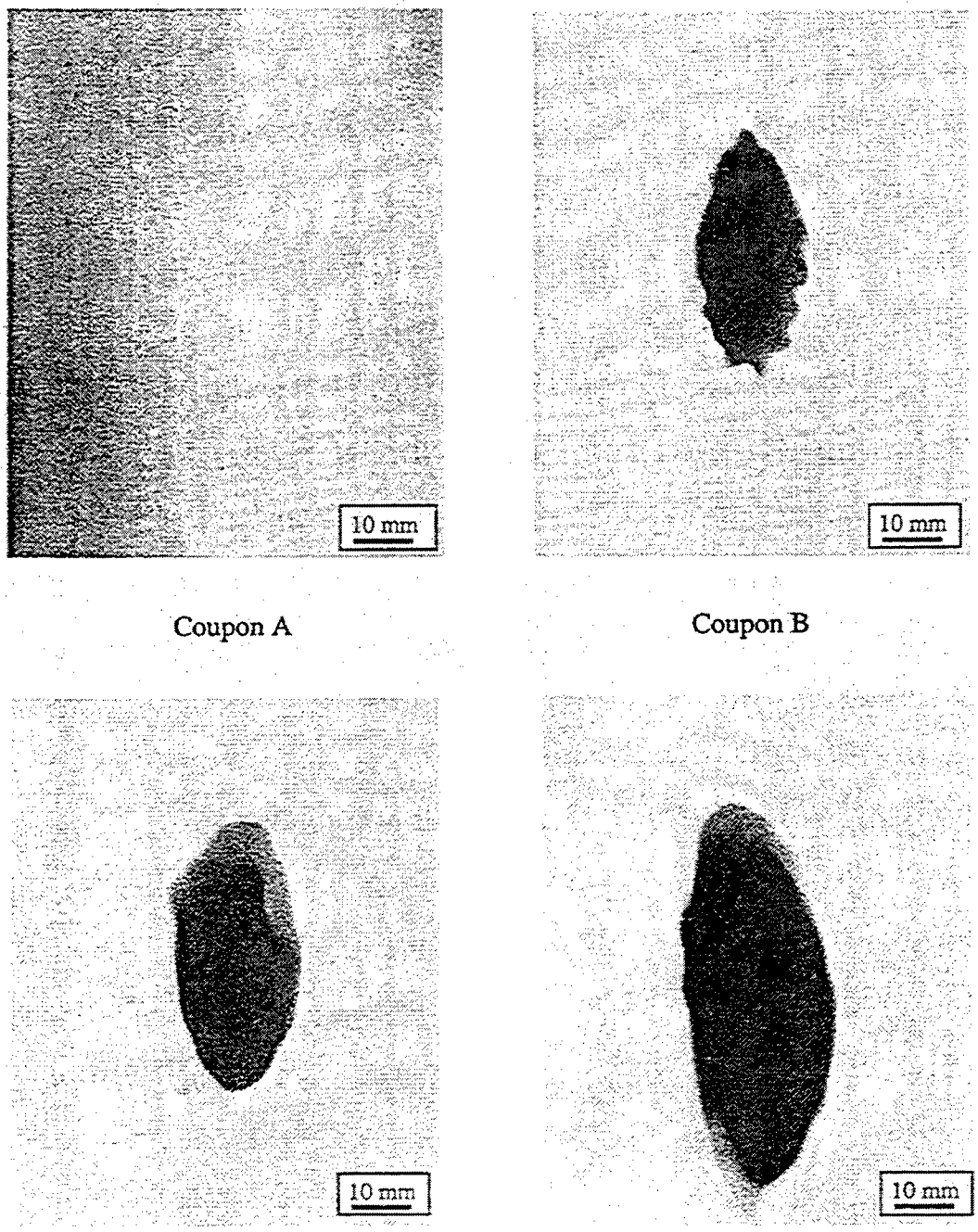

Figure 3.8-3. Phase maps of four impacted coupons (Richardson et al. 1998)

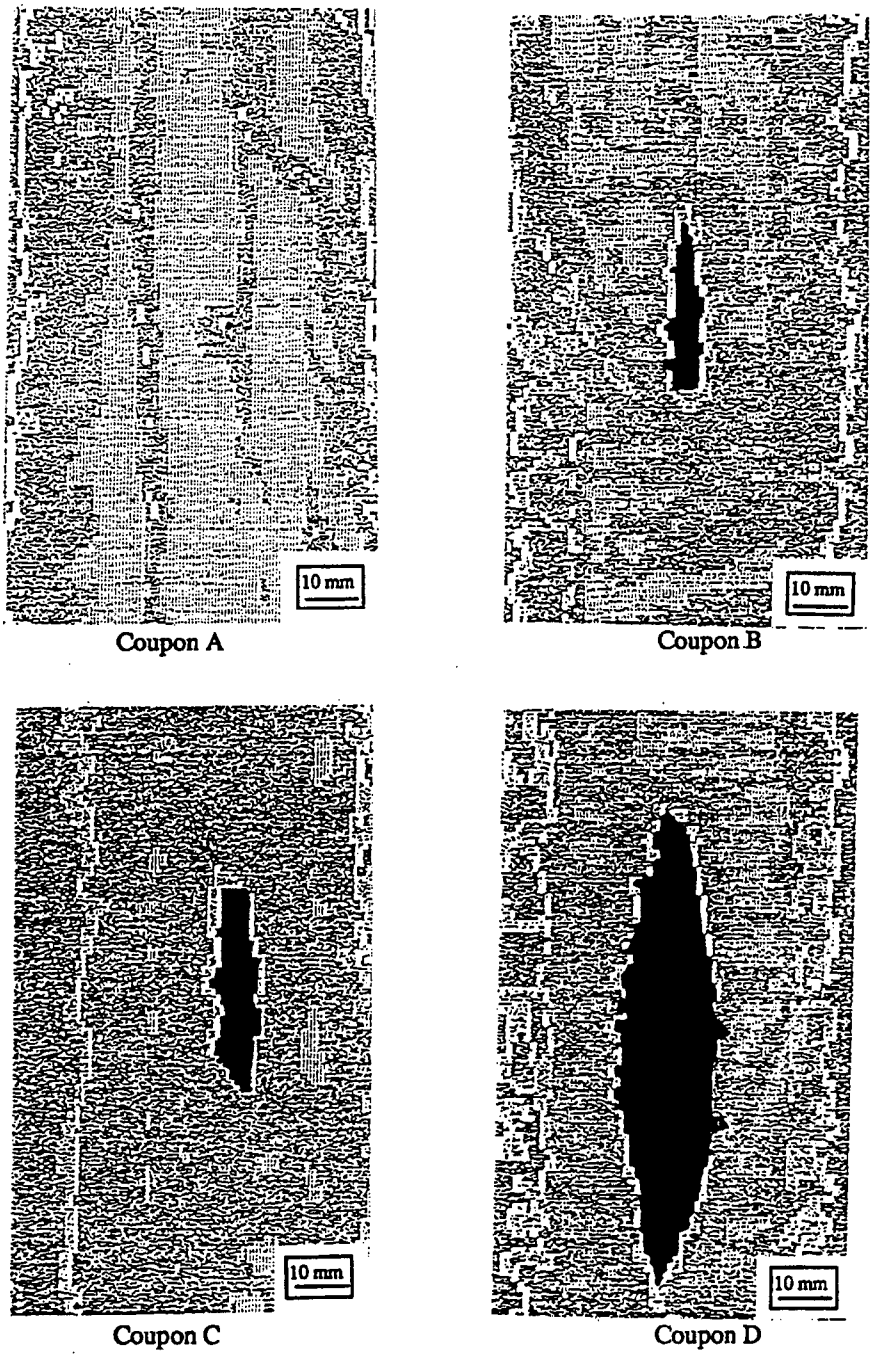

Figure 3.8-4. Damage profiles detected by ultrasonic c-scan (Richardson et al. 1998)

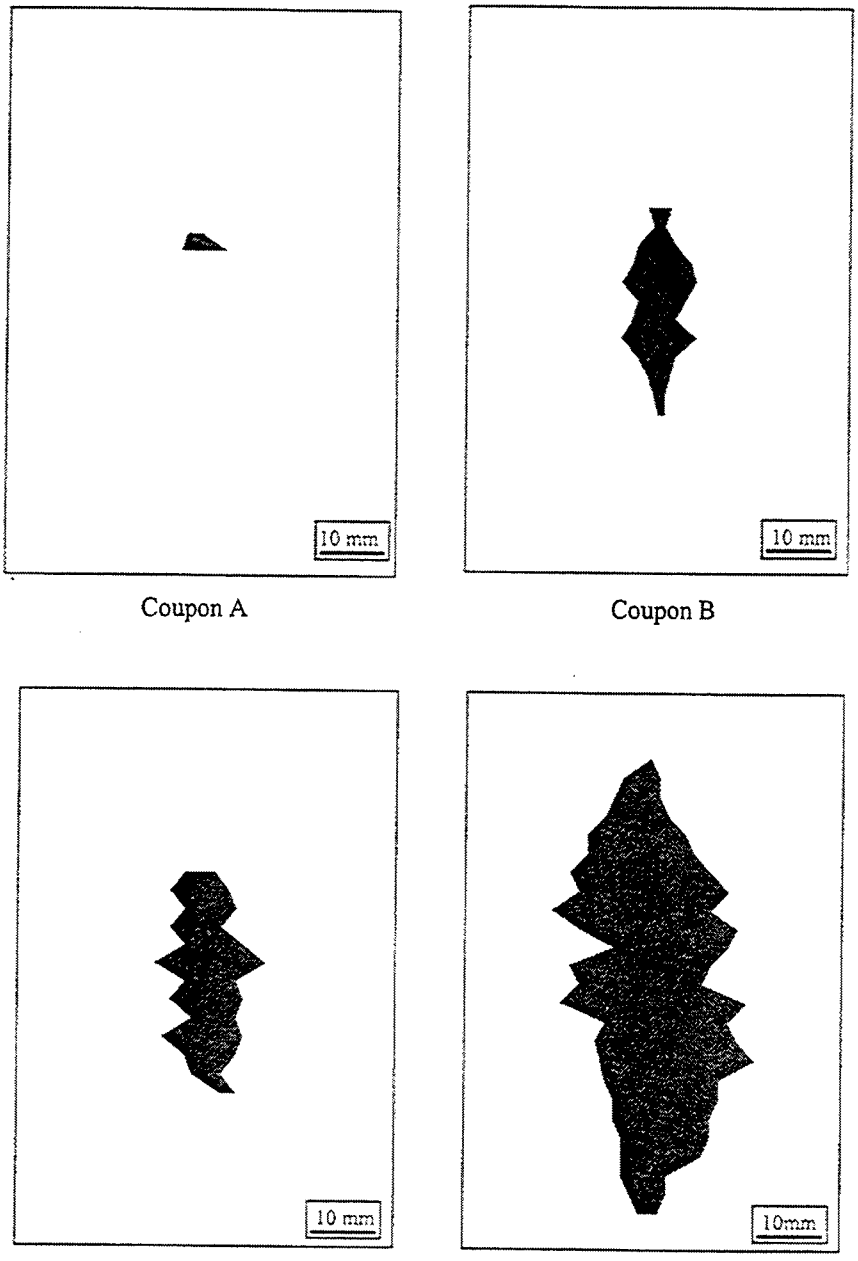

Figure 3.8-5. Damage profile of impacted coupons by sectioning technique (Richardson et al. 1998)

Table 3.8-1. Comparison of damage areas determined by intensity fringes, phase maps, ultrasonic C-scan and sectioning techniques. (Richardson et al. 1998)

Test technique	Damage area (mm^2)			
	Coupon A	Coupon B	Coupon C	Coupon D
Intensity fringe	0	188	256	9325
Phase map	0	194	270	975
C-scan	0	156	227	1168
Sectioning	0	223	330	1245

3.9 Thermal Conductivity

Thermal conductivity measurements of fiber reinforced polymer composites can be used to gain insight into potential NDE approaches. In particular in the case of hybrid composites, since they are relatively new, not all their properties are known. One of these areas is the effect of dual fiber reinforcement on the thermal response of the laminate.

Recently, Eihusen and Peters (1999) measured the transverse thermal conductivity of epoxy matrix composite panels with varying types of unidirectional fiber reinforcement. Twelve different flat panels of varying levels of hybridization of carbon, glass, and aramid fibers in an epoxy matrix were fabricated and tested. The test setup (following the general guidelines given in ASTM C518-91) was configured as a single-sided hot plate with an imbedded and guarded heat flux sensor (see Figure 3.9-1). A thermocouple imbedded in the face of the cold plate monitors the temperature response of the test sample.

The samples tested were flat panels of unidirectional reinforced epoxy composite. The panels were fabricated by filament winding a single 90° circumferential ply of composite material on a cylindrical mandrel. The uncured composite was then slit and removed from the mandrel. These composite mats were stacked to the required thickness and cured in a heated press. Shimming the press plates apart to a distance that would yield a composite fiber volume of approximately 60% controlled the final thickness of the composite panel.

The instrument thermocouple leads were monitored with an automatic datalogger. The datalogger was programmed to record the thermocouple temperatures every 10 seconds. Each sample was held in thermal equilibrium until the recorded temperatures had no more than a 1-degree deviation for the last 5 minutes of the sample run. The samples of dual fiber content were each subjected to three sampling runs.

The data indicate that for dual fiber hybrid composites with a fiber volume content of structural significance, the bulk transverse thermal conductivity of the laminate is a linear ratio of the percent of hybridization. It is of some note that the linear trend of the data for

the glass-carbon hybridization series displayed a perturbation of the measured response of the thermal conductivity of one of the samples. This sample had a measured thermal conductivity that was approximately 10% lower than its expected value over the three test runs. This anomaly could not be explained by instrument stabilization; therefore, Eihusen and Peters believe that the sample itself may hold several potential causes for this response.

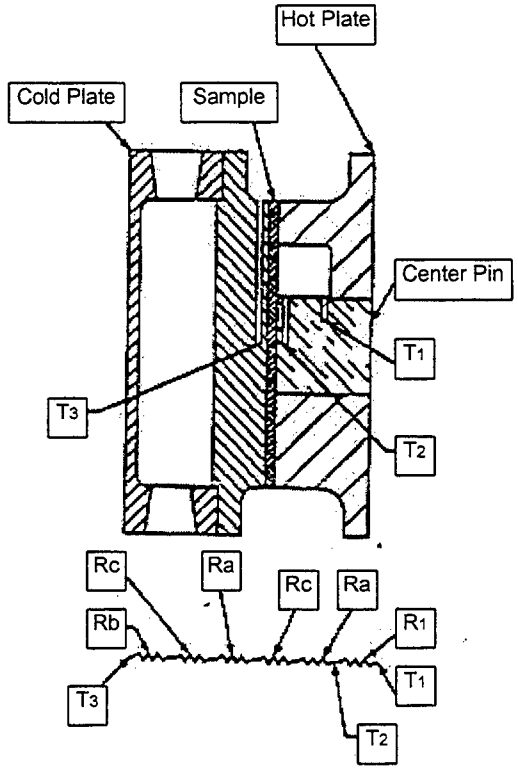

Figure 3.9-1. Thermal conductivity instrumentation assembly. (Eihusen and Peters 1999)

Eihusen and Peters believe they have provided sufficient data for future researchers to resolve potential calibration offsets of the muscovite mica standard used. This will allow the results of their effort to be comparatively matched or resolved against instrumentation yielding better absolute accuracy in thermal conductivity measurements. Their research also indicates that additional efforts would include characterization of the contact resistance of cured epoxy composites as a function of temperature.

4. CONCLUSIONS AND PROGNOSIS

Ultrasonic attenuation is probably the most widely used NDE method for assessing void content in CFRP (Hsu 1995). It is well known that porosity has pronounced effects on ultrasonic attenuation and wave velocity because the voids are strong scatterers for elastic waves. However, it is important to recognize that both attenuation and velocity are frequency dependent and it is necessary to take this dependence into account in order to obtain satisfactory correlation between ultrasonic measurement results and void content. In addition, a number of factors unrelated to porosity can contribute to the reduction of the ultrasonic signal amplitude, including diffraction loss due to beam spreading, interfacial transmission losses, and transducer frequency band characteristics. Therefore, certain measurement procedures and proper attention must be exercised in order to achieve a quantitative correlation between ultrasonic measurement results and porosity content.

The types of anomalies in graphite-epoxy composites that can be classified using ultrasonic scanning methods include thickness changes, fiber/matrix distribution, porosity content, contaminations, delaminations, and impact damage. In order for the ultrasonic pulse-echo C-scan imaging techniques to serve as a reliable tool for detecting and classifying defects in composites, a knowledge base has to be established based on samples with known parameters. This knowledge can then be used for statistical analysis, and data-reduction methods can be applied to speed up and reduce the cost of ultrasonic nondestructive evaluation of composites (Steiner 1992). Ultrasonic scanning methods need to be investigated further to determine if similar results can be achieved for glass-graphite hybrid composite materials.

Fecko et al. (1995) anticipate that by combining an in-process NDE porosity determination technique based on Lamb wave velocity measurements with process models to produce a process-control feedback loop will improve quality, reliability, and affordability of the thermoplastic pultrusion process.

Reis (1994a, 1994b) demonstrated that the acousto-ultrasonic approach allows the quantitative discrimination of different porosity levels in flange radii components, which are typical of complex structural parts made of advanced composite materials. While it is not clear what is the smallest defect the acousto-ultrasonic technique can detect, it appears that the presence of defects do significantly alter the waveform. Further studies must be pursued in this area for conclusive results.

Walker, et al. (1998) found that thermography was a good candidate for locating porosity that is close to the surface. When the porosity reached depths of six or more plies, they were not as confident that it could be detected without some surface preparation of the test object. By applying a flat black, water-washable paint, the porosity at the midplane of the panel could be detected. Additional research will need to be performed to develop methods to raise the sensitivity of the thermographic inspections to a level that will permit one-sided inspections without the need for altering the surface finish of a test object. Walker, et al. are continuing to investigate image enhancement to increase the

sensitivity of the thermographic system, optional heating methods to better excite the defect, and finite element methods to determine the theoretical limitations of the system.

A thermal technique for determining fiber volume fraction is advantageous since it is noncontacting, fast, and nondestructive. The thermal diffusivity measurement technique described by Zalameda and Winfree (1993) shows potential for estimating FVF nondestructively.

A dual technique of single-point diffusivity measurements and through-transmission ultrasonics has potential in nondestructively determining the fiber volume fraction (FVF) in cured composites (Zalameda and Smith 1994). An advantage of this technique is that no knowledge of the ply lay-up is required for the measurement.

Regular fiber lay-up can be quickly inspected using ultrasonic backscattering techniques. In a laboratory, backscattering can be used to evaluate the fiber directions of fractured sections during damage analysis (Schuster and Steiner 1993). Higher test frequencies and a smaller step-size combined with repeated measurements can increase the inspection quality but will also increase the inspection time.

Sullivan et al. (1996) showed that the plate wave flow pattern technique was successful in mapping the fiber directions of a multi-ply laminate. Their frequency filtering method showed that the potential for a ply-by-ply fiber orientation analysis exists, if suitable parameters are selected. Further theoretical background based on plate wave generation and propagation of plate waves in inhomogeneous plates must be developed and correlated with experimental data. Then a heuristic algorithm can be developed for a reliable method for ply orientation imaging.

Eddy current systems are not necessarily well suited for measurements on electrically conducting fiber reinforced polymer composites. The intrinsic inhomogeneity of composites, due to variations in fiber-fiber contacts and in the fiber volume fraction, may cause difficulties in distinguishing acceptable variations from defects. However, if these difficulties can be overcome, field applications and single-sided inspection are feasible, with the additional advantage that no couplant material is required (as is needed in ultrasonic methods).

Although X-ray radiography have proven reliable in determining fiber orientation in the laboratory and in industrial situations, x-ray radiography equipment and procedures are somewhat more difficult to apply in the field.

Microwave techniques are ill suited for composites containing carbon or graphite fibers because electrically conducting fibers strongly scatter the microwaves.

5. GLOSSARY AND ABBREVIATIONS

°	degrees
%	percent
A	
aramid	A manufactured fiber in which the fiber-forming substance is a long-chain synthetic aromatic polyamide in which at least 85% of the amide linkages are directly attached to two aromatic rings.
B	
bismaleimide	A type of polyimide that cures by an addition rather than a condensation reaction, thus avoiding problems with volatiles formation, and which is produced by a vinyl-type polymerization of a prepolymer terminated with two maleimide groups. Intermediate in temperature capability between epoxy and polyimide. Abbreviated BMI.
BMI	bismaleimide
C	
CFRP	carbon-fiber-reinforced plastic
cm	centimeter
cm^2/sec	square centimeters per second
compressive strength	The maximum stress that a material will bear when it is subjected to a load that pushes it together.
cure	To change the physical properties of an adhesive by chemical reaction, which may be condensation, polymerization, or vulcanization; usually accomplished by the action of heat and catalyst, alone or in combination, with or without pressure.
D	
dB	decibel
diffusion	The process whereby particles of liquids, gases, or solids intermingle as the result of their spontaneous movement caused by thermal agitation and in dissolved substances move from a region of higher to one of lower concentration.
E	
epoxy	A thermoset polymer containing one or more epoxide groups and curable by reaction with amines, alcohols, phenols, carboxylic acids, acid anhydrides, and mercaptans. Epoxy plastics are an important matrix resin in reinforced composites and in structural adhesives.
F	
FFT	fast Fourier transform
fiberglass	A composite material made of fine glass fibers woven into a cloth then bonded together with a synthetic plastic or resin.
FVF	fiber volume fraction

G	
GRP	glass-reinforced plastic
H	
heterogeneity	The quality or state of being heterogeneous.
heterogeneous	Consisting of dissimilar or diverse ingredients or constituents.
Hz	hertz
J	
J/(cm^3-°C)	joules per cubic centimeter per degree Celsius
M	
matrix	The part of an adhesive that surrounds or engulfs embedded filler or reinforcing particles and filaments.
matrix-rich	see resin-rich area
matrix-starved	see resin-starved area
MHz	megahertz
microstructure	A structure with heterogeneities that can be seen through a microscope.
mm	millimeter
monomer	A single molecule that can react with like or unlike molecules to form a polymer. The smallest repeating structure of a polymer (mer).
N	
NDE	nondestructive evaluation
NDI	nondestructive inspection
P	
PAN	polyacrylnitrile
plastics	Solid materials consisting of organic polymers.
polyamide	A thermoplastic polymer in which the structural units are linked by amide or thio-amide groupings (repeated nitrogen and hydrogen groupings). Many polyamides are fiber forming.
polyimide	A polymer produced by reacting an aromatic dianhydride with an aromatic diamine. It is a highly heat-resistant resin. It is similar to a polyamide, differing only in the number of hydrogen molecules contained in the groupings. This polymer is suitable for use as a binder or adhesive and may be either a thermoplastic or a thermoset.
polymer	Polymers are large molecules that are made up of many units (monomers) linked together in a chain. There are naturally occurring polymers (e.g., starch and DNA) and synthetic polymers (e.g., nylon and silicone).

polyurethanes	A large family of polymers with widely varying properties and uses. All of these polymers are based on the reaction product of an organic isocyanate with compounds containing a hydroxyl group. Polyurethanes may be thermosetting or thermoplastic, rigid or soft and flexible, cellular or solid. The properties of any of these types may be tailored within wide limits to suit the desired application.
porosity	A condition of trapped pockets of air, gas, or vacuum within a solid material. Usually expressed as a percentage of the total nonsolid volume to the total volume (solid plus nonsolid) or a unit of quantity of material.
prepreg	A fiber-reinforced composite laminate structure made by bonding and curing two or more layers of material.
pultrusion	A continuous molding process that mechanically aligns long strands of reinforcements for a composite material, then passes them through a bath of thermosetting resin. The coated strands are then assembled by a mechanical guide before the curing process.
R	
resin-rich area	Localized area filled with resin and lacking reinforcing material.
resin-starved area	Localized area of insufficient resin, usually identified by low gloss, dry spots, or fiber showing on the surface.
S	
S/m	siemens per meter
stress	Force per unit area. Stress is measured in the same units as pressure, namely pascals (Pa). Materials typically have strengths in the megapascal (MPa) range (1 MPa = 1,000,000 Pa).
SWF	stress wave factor
T	
tensile strength	The maximum stress a material will bear when it is subjected to a stretching load.
V	
vinyl esters	A class of thermosetting resins containing esters of acrylic and/or methacrylic acids, many of which have been made from epoxy resin. Cure is accomplished, as with unsaturated polyesters, by copolymerization with other vinyl monomers, such as styrene.
W	
W/(cm-°C)	watts per centimeter per degree Celsius

6. REFERENCES

Akers, David, Chris Vaccaro, Skip Ellsworth, and Don Pettit. "The Effect of Porosity Density and Configuration in Composite Materials on the Ultrasonic Waveform." Review of Progress in Quantitative Nondestructive Evaluation, Vol. 15. Edited by Donald O. Thompson and Dale E. Chimenti. New York: Plenum Press. 1996. pp. 1239-1246.

Bai, W., and B.S. Wong. "Evaluation of Defects in Composite Plates Under Convective Environments Using Lock-in Thermography." *Measurement Science and Technology, Vol. 12*, Institute of Physics Publishing, 2001, pp. 142-150.

Ball, R.J., and D.P. Almond. "The Detection and Measurement of Impact Damage in Thick Carbon Fibre Reinforced Laminates by Transient Thermography." *NDT&E International, Vol. 31, No. 3*. Elsevier Science, Ltd. 1998. pp. 165-173.

Chun, H.J., and P.S. Jang. "Nondestructive Evaluation of Degree of Fiber Waviness in Thick Composites." *Key Engineering Materials*, Vols. 183-187. 2000 Trans Tech Publications, Switzerland, 2000. pp. 1069-1074.

Clarke, A. R., G. Archenhold and N. C. Davidson. "A Novel Technique for Determining the 3D Spatial Distribution of Glass Fibres in Polymer Composites." Composites Science and Technology, vol. 55. 1995. pp. 75-91.

de Goeje, M. P., and K. E. D. Wapenaar. "Non-Destructive Inspection of Carbon Fibre-Reinforced Plastics Using Eddy Current Methods." Composites, vol. 23, no. 3. May 1992. pp. 147-157.

Eihusen, John A., and Alexander R. Peters. "Characterization of the Transverse Thermal Conductivity of Intraply Hybrid Composite Laminates." Proceedings of the 1999 31st International SAMPE Technical Conference: Advanced Materials and Processes Preparing for the New Millennium. Society for the Advancement of Material and Process Engineering (SAMPE). 1999. pp. 211-220.

Elvin, Niell, and Christopher Leung. "Feasibility Study of Delamination Detection with Embedded Optical Fibers." *Journal of Intelligent Material Systems and Structures, Vol. 8*. Technomic Publishing Co., Inc. 1998. pp. 824-828.

Fecko, David L., Dirk Heider, John W. Gillespie, Jr., and Karl V. Steiner. "In-Process Non-Destructive Evaluation of the Pultrusion Process." Nondestructive Evaluation of Aging Aircraft, Airports, Aerospace Hardware, and Materials, SPIE, Volume 2455. Edited by Tobey M. Cordell and Raymond D. Rempt. The International Society for Optical Engineering (SPIE). 1995. 280-290.

Fecko, D. L., J. W. Gillespie, Jr., and K. V. Steiner. "Use of Ultrasonic Lamb Waves for In-Process Porosity Inspection of the Pultrusion Process: Theoretical Velocity Calculations." Review of Progress in Quantitative Nondestructive Evaluation, Vol. 15B. Edited by Donald O. Thompson and Dale E. Chimenti. New York: Plenum Press. 1996. pp. 1231-1238.

Gottesman, T., and S. Girshovich. "Impact Damage Assessment and Mechanical Degradation of Composites." *Key Engineering Materials, Vols. 141-143.* Trans Tech Publications, Switzerland. 1998. pp. 3-18.

Gray, Sheila, Stoyan Ganchev, Nasser Qaddoumi, Guy Beauregard, Donald Radford, and Reza Zoughi. "Porosity Level Estimation in Polymer Composites Using Microwaves." Materials Evaluation, vol. 53, no. 3. 1995. pp. 404-408.

Gros, Xavier E., "Current and Future Trends in Nondestructive Testing of Composite Materials." *Ann. Chim. Sci. Mat., 2000. 25.* pp. 539-544.

Gros, X.E., and K. Takahashi. "Nondestructive Characterization of Delaminated Areas at Interfaces Between Plies in Carbon Fiber/Epoxy Laminates with Foucalt Currents." *Composite Interfaces, Vol. 7, No. 3.* VSP. 2000. pp. 177-192.

Hesiehurst, R.B., J.P. Baird, and H.M. Williamson. "Location and Direction of the Propagation of an Existing Delamination in Composite Panels." *Journal of Advanced Materials, Vol. 30, No. 3.* 1998. pp. 38-43.

Hsu, D. "Ultrasonic Nondestructive Evaluation of Void Content in CFRP." ANTEC '88, Proceedings of the 46th Annual Technical Conference. 1988. pp. 1273-1275.

Hsu, David K. "Ultrasonic Methods for Evaluating Porosity Content and Mechanical Strength of CFRP Laminates." NDE of Composites and Composite Materials. ASNT 1995 Spring Conference, Fourth Annual Research Symposium, March 20-24, 1995. Columbus, Ohio: American Society for Nondestructive Testing (ASNT). 1995. p.223.

Joyce, Peter J., Danielle Kugler and Tess J. Moon. "A Technique for Characterizing Process-Induced Fiber Waviness in Unidirectional Composite Laminates-Using Optical Microscopy." Journal of Composite Materials. vol. 31, no. 17. 1997. pp. 1694-1727.

Karabutov, Alexander A., V. V. Murashov, Natalia B. Podymova, and Alexander A. Oraevsky. "Nondestructive Characterization of Layered Composite Materials with a Laser Optoacoustic Sensor." Nondestructive Evaluation of Materials and Composites II, SPIE, Volume 3396. Edited by Steven R. Doctor, Carol A. Lebowitz, and George Y. Baaklini. The International Society for Optical Engineering (SPIE). 1998. pp. 103-111.

Kline, Ronald A. "Ultrasonic Characterization of Composite Microstructure." Nondestructive Characterization of Materials IV. Edited by Clayton O. Ruud, Jean F. Bussiere, and Robert E. Green, Jr. New York: Plenum Press. 1991. pp. 321-328.

Liu, John M. "Microwave and Ultrasonic NDE of Thick Glass-Fiber-Reinforced Composites." Nondestructive Evaluation of Materials and Composites II, SPIE, Volume 3396. Edited by Steven R. Doctor, Carol A. Lebowitz, and George Y. Baaklini. The International Society for Optical Engineering (SPIE). 1998. pp. 135-139.

McRae, Kenneth I., and Cedric A. Zala. "Attenuation and Porosity Estimation Using the Frequency-Independent Parameter Q." Review of Progress in Quantitative Nondestructive Evaluation, Vol. 14A. Edited by Donald O. Thompson and Dale E. Chimenti. New York: Plenum Press. 1995. pp. 703-710.

Michaeli, Walter, Karsten Brast, and Markus Piry. "Non-Destructive Measurement of Fibre Orientation." Kunststoffe Plast Europe, vol. 89, no. 9. September 1999. pp. 45-46.

Mol, G. W. "Automatic Estimation of Fibre Orientation of Cured CFRP by Image Processing of High Resolution Ultrasonic Pulse-Echo Images." Non-Destructive Testing 92, Edited by C. Hallai and P. Kulcsar, Elsevier Science Publishers B.V. 1992. pp. 979-983.

Mouritz, A.P., C. Townsend, and M.Z. Shah Khan. "Nondestructive Detection of Fatigue Damage in Thick Composites by Pulse-Echo Ultrasonics." *Composites Science and Technology*. Elsevier. 2000. pp. 23-32.

Park, Joong-Wan, Chi-Young Ryu, Hyun-Kyu Kang, and Chang-Sun Hong. "Detection of Buckling and Crack Growth in the Delaminated Composites Using Fiber Optic Sensor." *Journal of Composite Materials, Vol. 34, No. 19/2000*. Technomic Publishing Co., Inc. 2000. pp. 1602-1623.

Reis, Henrique. "Acousto-Ultrasonic Nondestructive Evaluation of Porosity in Graphite Fiber Reinforced PMR-15 Composite Panels." International Advances Nondestructive Testing, Volume 17. Edited by Warren J. McGonnable. Langhorne, Pennsylvania: Gordon and Breach Science Publishers. 1994a. pp. 339-356.

Reis, Henrique L. M. dos. "Acousto-Ultrasonic Nondestructive Evaluation of Porosity in Polymer-Composite Structures of Complex Geometry." Journal of Acoustic Emission, vol. 12, no. 1/2. January-June 1994. Acoustic Emission Group. 1994b.pp. 15-21.

Richardson, M.O.W., Z.Y. Zhang, M. Wisheart, J.R. Tyrer, and J Petzing. "ESPI Nondestructive Testing of GRP Composite Materials Containing Impact Damage." *Composites, Part A 29A*. Elsevier Science, Ltd. 1998. pp. 721-729.

Scarponi, C., and G. Briotti. "Ultrasonic Technique for the Evaluation of Delaminations on CFRP, GFRP, KFRP Composite Materials." *Composites, Part B: Engineering*. Elsevier. 2000. pp. 237-243.

Schuster, Jens, and Karl V. Steiner. "Ultrasonic Backscattering Using Digitized Full-Waveform Scanning Technique." Journal of Composites Technology and Research, vol. 15, no. 2. Summer 1993. American Society for Testing and Materials (ASTM). pp. 143-148.

Sirkis, J.S., Chang, C.C., and Smith, B.T. "Low Velocity Impact of Optical Fiber Embedded Laminated Graphite/Epoxy Panels. Part I: Macro Scale." *Journal of Composite Materials, Vol. 28, No. 14/1994*. Technomic Publishing Company, Inc. 1994. pp. 1347-1370.

Smith, R.A., A.B. Marriott, and L.D. Jones. "Delamination Sizing in Fibre-Reinforced Plastics Using Pulse-Echo Amplitude." *Insight, Vol. 39, No. 5*. May 1997. pp. 330-336.

Steiner, Karl V. "Defect Classifications in Composites Using Ultrasonic Nondestructive Evaluation Techniques." Damage Detection in Composite Materials, STP 1128. Edited by John E. Masters. Philadelphia, Pennsylvania: American Society for Testing and Materials (ASTM). 1992. pp. 72-84.

Sullivan, Rani Warsi, Krishnan Balasubramaniam, and George Bennett. "Plate Wave Flow Patterns for Ply Orientation Imaging in Fiber Reinforced Composites." Materials Evaluation, vol. 54, no. 4. April 1996. pp. 518-523.

Todoroki, Akira, Hideo Kobayashi, and Katsuya Matsuura. "Application of Electric Potential Method to Smart Composite Structures for Detecting Delamination." *Proceedings of ICCM-10*, Whistler, B.C. Canada. August 1995. pp. V323-V330.

Walker, James L., Samuel S. Russell, and Gary L. Workman. "Thermographic Qualification of Graphite/Epoxy Instrumentation Racks." Nondestructive Evaluation of Aging Aircraft, Airports, and Aerospace Hardware II, SPIE, vol. 3397. The International Society for Optical Engineering (SPIE). 1998. pp. 141-148.

Wang, Xiaojun, and D.D.L. Chung. "Sensing Delamination in a Carbon Fiber Polymer-Matrix Composite During Fatigue by Electrical Resistance Measurement." Polymer Composites, Vol. 18, No. 6. 1997. pp. 692-700.

Wooh, Shi-Chang, and Isaac M. Daniel. "Characterization of Fiber Waviness in Thick Composites Based on an Ultrasonic Ray Tracing Model." *Review of Progress in Quantitative Nondestructive Evaluation, Vol. 13.* Edited by D.O. Thompson and D.E. Chimenti, Plenum Press, New York, 1994. pp. 1291-1298.

Zalameda, Joseph N. and Barry T. Smith. "Measurement of Composite Fiber Volume Fraction Using Thermal and Ultrasonic Inspection Techniques." Nondestructive Characterization of Materials VI. Edited by R. E. Green, Jr., Krzysztof J. Kozaczek, and Clayton O. Ruud. New York: Plenum Press. 1994. pp. 741-748.

Zalameda, Joseph N., Gary L. Farley, and Barry T. Smith. "A Field Deployable Nondestructive Impact Damage Assessment Methodology for Composite Structures." *Journal of Composites Technology & Research.* pp.161-169.

Zalameda, Joseph N. and William P. Winfree. "Quantitative Thermal Diffusivity Measurements on Composite Fiber Volume Fraction (FVF) Samples." Review of Progress in Quantitative Nondestructive Evaluation, Vol. 12B. Edited by Donald O. Thompson and Dale E. Chimenti. New York: Plenum Press. 1993. pp. 1289-1295.

7. BIBLIOGRAPHY

Balageas, Daniel L., Nicolas Jaroslavsky, Marc Dupont, Francois Lepoutre, and Daniel Osmont. "Laser Generated Lamb Waves in Carbon/Epoxy Composite Structures Using an Embedded Fiber Optic Delivery System." Smart Structures and Materials 2000: Smart Structures and Integrated Systems. SPIE Vol. 3985. 2000. pp. 543-550.

Ben Jar, P.Y., X.E. Gros, K. Takahashi, K. Kawabata, J. Murai, and Y. Shinagawa. "Evaluation of Delamination Resistance of Glass Fibre Reinforced Polymers Under Impact Loading." Journal of Advanced Materials, Volume 32, No. 3. July 2000. Pp. 35-45.

Bourasseau, Serge, Marc Dupont, Daniel Balageas, Eric Bocherens, Veronique Dewynter-Marty, and Pierre Ferdinand. "Impact Damage Detection in Radome Sandwich Structures by Traditional Non Destructive Evaluation and Fiber Optic Integrated Health Monitoring Systems." Proceedings of the Tenth International Conference on Adaptive Structures and Technologies. Technomic. October 1999. pp. 436-443.

Chen, Zao, Victor Giurgiutiu, Craig A. Rogers, Robert Quattrone, and Justin Berman. "Improved Active Tagging Non-Destructive Evaluation Techniques for Full-Scale Structural Composite Elements." Proceedings of International Composites Expo '97. Paper 68. January 1997. pp. 1-6.

Chien, Hual-Te, Shuh-Haw Sheen, and Apostolos C. Raptis. "An Acousto-Ultrasonic NDE Technique for Monitoring Material Anisotropy." Review of Progress in Quantitative Evaluation, Vol. 12. Edited by D.O. Thompson and D.E. Chimenti. Plenum Press. New York. 1993. pp.1225-1232.

De Goeje, M.P. and K.E.D. Wapenaar. "Non-Destructive Inspection of Carbon Fibre-Reinforced Plastics Using Eddy Current Methods." Composites, Vol. 23, No. 3. May 1992. pp. 147-157.

Doyum, A. Bulent, and Balkar Altay. "Detection of Low-Velocity Impact Damage in Glass/Epoxy Tubes by the Penetrant Method." Insight, Vol. 40, No. 2. February 1998. pp.117-121.

Fahr, A., C.E. Chapman, J.F. Laliberte, D.S. Forsyth, and C. Poon. "Nondestructive Evaluation Methods for Damage Assessment in Fiber-Metal Laminates." Polymer Composites, Vol. 21, No. 4. August 2000. pp. 568-575.

Fahr, A., C.E. Chapman, J.F. Laliberte, D.S. Forsyth, and C. Poon. "Nondestructive Evaluation Methods for Damage Assessment in Fiber-Metal Laminates." Polymer Composites, Vol. 21, No. 4. August 2000. pp. 568-575.

Gomes, J.F. Silva, J.M. Monteiro, and M.A.P. Vaz. "NDI of Interfaces in Coating systems Using Digital Interferometry." Mechanics of Materials 32. Elsevier. 2000. pp. 837-843.

Green, William H., and Joseph M. Wells. "Nondestructive Characterization of Impact Damage in Metallic/Nonmetallic Composites Using X-ray Computed Tomography Imaging." Army Research Laboratory. ARL-TR-2399. February 2001.

Green, William H., and Patrick Sincebaugh. "Nondestructive Evaluation of Complex Composites Using Advanced Computed Tomography (CT) Imaging." Army Research Laboratory. ARL-TR-2400. February 2001.

Haque, A., U.K. Vaidya, H. Mahfuz, and S. Jeelani. "Nondestructive Evaluation (NDE) of Thick Section Composites Under Static Compression and Compression-Compression Cyclic Loading." 14th World Conference on Non Destructive Testing. New Delhi, India. December 1996. pp. 529-533.

Hsu, David K. and Brent A. Fischer. "Inspection of Composite Laminate Lay-up Using Shear Ultrasonic Waves." 41st International SAMPE Symposium. Society for the Advancement of Material and Process Engineering. 1996. pp. 597-608.

Komsky, I.N., I.M. Daniel, and Y.C. Lee. "Ultrasonic Determination of Layer Orientation in Multi-layer Multidirectional Composite Laminates." Review of Progress in Quantitative Evaluation, Vol. 11. Edited by D.O. Thompson and D.E. Chimenti. Plenum Press. New York. 1992. pp. 1615-1622.

Komsky, I.N., K. Zgonc, and I.M. Daniel. "Ultrasonic Determination of Layer Orientation in Composite Laminates Using Adaptive Signal Classifiers." Review of Progress in Quantitative Evaluation, Vol. 13. Edited by D.O. Thompson and D.E. Chimenti. Plenum Press. New York. 1994. pp.787-794.

Krapez, J.C. "Thermal Ellipsometry: A Tool Applied for In-Depth Resolved Characterization of Fibre Orientation in Composites." Review of Progress in Quantitative Evaluation, Vol. 15. Edited by D.O. Thompson and D.E. Chimenti. Plenum Press. New York. 1996. pp. 533-540.

Krzesinska, M., A. Celzard, J.F. Mareche, and S. Puricelli. "Elastic Properties of Anisotropic Monolithic Samples of Compressed Expanded Graphite Studied with Ultrasounds." Journal of Materials Research, Vol. 16, No. 2. Materials Research Society. February 2001. pp. 606-614.

Marti, David K., Gene J. Descant, and Steven M. Craig. "Apparatus and Method for Performing Non-Destructive Inspections of Large Area Aircraft Structures." US Patent No. US 6,220,099 BI. April 24, 2001.

Mistou, S., and M. Karama. "Determination of the Elastic Properties of Composite Materials by Tensile Testing and Ultrasound Measurement." Journal of Composite Materials, Vol. 34, No. 20/2000. Technomic Publishing Co., Inc. 2000.

Modderman, T.M., and P.A.A.M. Somers. "Non-Destructive Determination of Stack Sequence of Carbon Fiber Reinforced Plastics." Non-Destructive Testing 92. Edited by C. Hallai and P. Kulcsar. Elsevier Science Publishers B.V. 1992. pp. 1201-1205.

Pastorius, Walt. "Vision Based Large Area Inspection of Composite Surfaces." SAMPE-ACCE-DOE Advanced Composites Conference, September 27-28, 1999. pp. 338-343.

Potel, Catherine, Thierry Chotard, Jean-Francois de Belleval, and Malk Benzeggagh. "Characterization of Composite Materials by Ultrasonic Methods: Modelization and Application to Impact Damage." Composites, Part B, 29B. Elsevier Science Ltd. 1998. pp. 159-169.

Ramamurthy, A.C., T. Ahmed, L.D. Favro, R.L. Thomas, and David K. Hsu. "Low Velocity Foreign Object (FOD) Damage to Composites and Automotive Paint Finishes: A Thermal Wave Study." Review of Progress in Quantitative Nondestructive Evaluation, Vol. 13. Edited by D.O. Thompson and D.E. Chimenti: Plenum Press, New York. 1994. pp.455-460.

Reis, Henrique. "Nondestructive Evaluation of Porosity in Polymer Matrix Composites. "Second International Conference on Acousto-Ultrasonics. ASNT. June 1993. pp. 107-116.

Roth, Don J. "Using a Single Transducer Ultrasonic Imaging Method to Eliminate the Effect of Thickness Variation in the Images of Ceramic and Composite Plates." Journal of Nondestructive Evaluation, Vol. 16, No. 2. Plenum Publishing Corporation. 1997. pp. 101-120.

Rudolph, H.V., H. Ivers, and K.W. Harbich. "Application of X-ray Refraction Topography to Fibre Reinforced Plastics." Composites: Part A, Applied Sciences and Manufacturing. Vol. 32. 2001. pp. 473-476.

Steiner, K.V. "Volumetric Visualization of Ultrasonic NDE of Composite Laminates." Proceedings of the American Society for Composites, Ninth Technical Conference. Technomic Publishing Co. Inc. 1994. pp. 238-245.

Steiner, Karl V., and Timothy C. Linday. "Correlation of Full-Waveform Ultrasonic NDE Data and Low-Velocity Impact Damage to Composite Panels." Review of Progress in Quantitative Nondestructive Evaluation, Vol. 13. Edited by D.O. Thompson and D.E. Chimenti. Plenum Press. New York. 1994. pp.1283-1290.

Steiner, Karl V., Knut Krieger, James B. Mehl, James N. Caron, and Yuqiao Yang. "Infrared Thermography and Laser-Based Ultrasonic Methods for On-Line Porosity Sensing During Thermoplastic Composites Fabrication." Proceedings from the Second Conference on NDE Applied to Process Control of Composite Fabrication. October 1996. pp. 115-121.

Sullivan, R., K. Balasubramaniam, A.G. Bennett, and C.A. Issa. "Experimental Imaging of Fiber Orientation in Multi-Layered Graphite Epoxy Composite Structures." Review of Progress in Quantitative Evaluation, Vol. 13. Edited by D.O. Thompson and D.E. Chimenti. Plenum Press. New York. 1994. pp. 1313-1320.

Tomblin, John S., K.S. Raju, J. Liew, and B.L. Smith. "Impact Damage Characterization and Damage Tolerance of Composite Sandwich Airframe Structures." Department of Transportation, Federal Aviation Administration. Report No. DOT/FAA/AR-00144. 2001.

Zalameda, Joseph N., and William P. Winfree. "Thermal Imaging of Graphite/Epoxy Composite Samples with Fabricated Defects." Review of Progress in Quantitative Evaluation, Vol. 10A. Edited by D.O. Thompson and D.E. Chimenti. Plenum Press. New York. 1991. pp. 1065-1072.

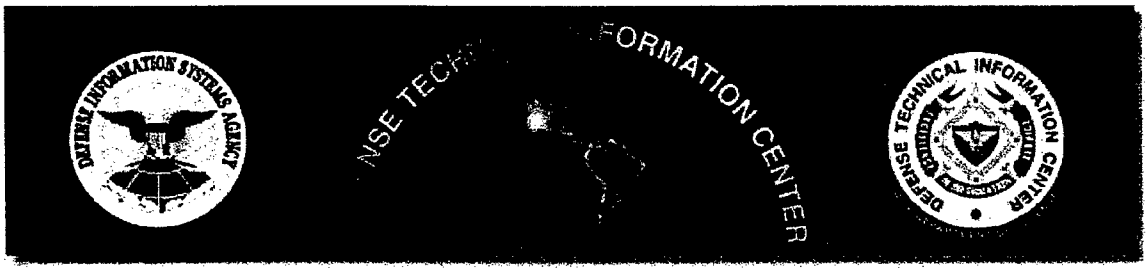

Defense Information Systems Agency
Defense Technical Information Center
8725 John J. Kingman Road, Suite 0944
Ft. Belvoir, VA 22060-6218

http://www.dtic.mil